UNIVERSITY OF WEST FLORIDA

2023-2024 DESIGN REPORT

AIAA DESIGN/BUILD/FLY COMPETITION

Table of Contents

1. Executive Summary

This report documents the design, manufacturing, and testing of the University of West Florida's Design/Build/Fly competition radio controlled plane. The plane named "The Scorpion" is competing in the 2023-24 Design/Build/Fly competition. The plane is designed, built, and tested by The University of West Florida's DBF seven undergraduate member team. The design requirements for the competition aircraft provided by the design and mission requirements stated by AIAA are set out in 4 missions [1]. Three of the missions are flight missions, where the plane must fly a predetermined flight path holding cargo. For Mission 1 the flight consists of three laps around the flight path while carrying the pilots as the only cargo. Mission 2 requires crew, EMTs, one patient on a gurney, and a medical supply cabinet. The flight for Mission 2 is to traverse the flight path three times in the shortest amount of time. Mission 3 will carry 2 pilots and 12 passengers along a predetermined flight path in a 5-minute time frame. Mission 3 requires the plane to fly along the flight path and make as many laps as possible within the time frame. The ground mission will be a timed activity for a member of the team to change to every mission configuration. The major design constraint for this competition year is that the plane must fit within a parking space 2.5 feet wide. The plane must fit while not having any components to be taken off the aircraft.

The Scorpion is driven by a singular tractor motor configuration mounted at the front of the aircraft. The maximum static thrust of the motor being used is 5.29 lbs. The highest gross takeoff weight is 4.86 lbs during Mission 2. This gives the aircraft a thrust to weight ratio of 1.09. The thrust to weight ratio gives the plane adequate space to take off within the 20ft take-off distance. The low wing configuration enables the changing time between mission configurations during the ground mission to be reduced due to easy access to the hatch on the side of the plane. The length of the wingspan is 5 feet to utilize the most amount of wing surface to contribute to lift. The shape of the wing is rectangular for its high lift and good stall characteristics. The empennage is a conventional configuration to provide lower drag and adequate space for the 3 flight mission requirements. The empennage conventional design made folding the rear portion of the fuselage up during parking more structurally resilient by utilizing a strong hinge attached on the top section of the fuselage of the aircraft.

The Scorpion was designed, manufactured, and tested by a 7 member team of Mechanical Engineering majors. The team is split up into subteams to directly tackle large portions of the project. The team utilized sensitivity analyses and trade studies to determine the components that best fit the mission requirements. The structures sub-team is responsible for 3D-printing components, composite molding, and joining all the components together. The plane is made from carbon fiber components, aluminum rods, and balsa wood to keep individual components weights low. Before prototypes are made small test components are made to test and ensure the validity of the team's calculations on a smaller scale. Three prototypes were made to provide ground and flight testing to iteratively improve the aircraft performance.

The goal for the University of West Florida DBF team is to achieve the highest score of the competition for all 4 missions and final report. The estimated ground mission time was calculated to be 120 seconds. For Mission 2, the plane will carry a medical supply cabinet with a weight of 0.5 lbs to ensure a safe takeoff within the 20 foot limitation. Then for Mission 3, 12 passengers will be flown. To decrease the time for each mission, the Dualsky V2 motor will propel the plane to exceed over 30 miles per hour.

2. Management Summary

The University of West Florida's DBF team consists of 7 members majoring in Mechanical Engineering. The team is split up into 4 seniors and 3 sophomores/ juniors. Each member has a specific area of responsibility to their subteam and for documentation for their respected subteam. A Gantt chart was created early on in the design process to ensure the project followed a scheduled deadline system.

2.1 Team Organization

The team consists of 5 seniors and 3 sophomores all working towards Bachelor of Science in Mechanical Engineering degrees. The team is divided into separate sub-teams to maximize efficiency. The team is divided into 4 main categories along with a team lead. The 4 main categories are budget, aerodynamics, electronics and propulsion, and structures as shown in Figure 1. Each subgroup is required to document and write about their respective expertise. Each sub-group's main
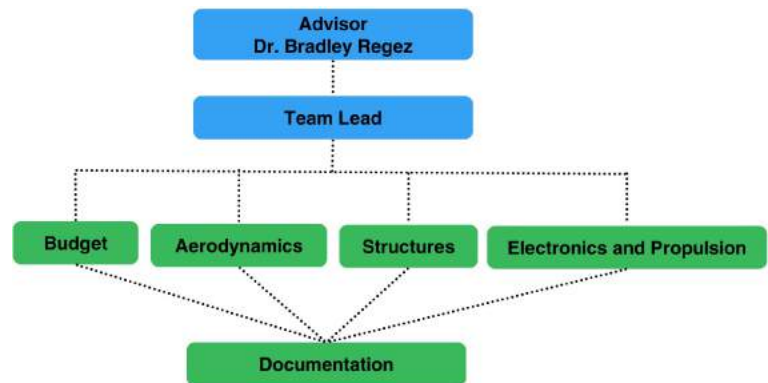

Figure 1: Team Structure

responsibilities and required skills are shown in Table 1. The aerodynamic subteam must ensure that the wing is designed to provide the lift necessary to meet the takeoff distance limitation. Part of this entails creating performance simulations to predict the plane's behavior. The wing must also be designed to provide ease of control to the pilot, which requires knowledge of aircraft stability and balance. Analysis and decisions relating to airfoil selection, wing and tail sizing, and stability are the responsibility of the aerodynamics subteam. The structures sub-team consists of designing, building, and testing structural components of the aircraft. The subteams determine what tasks need to be done, then present them to the team lead. The team lead

Table 1: Sub-Team Responsibilities and Skillset

Sub Team	Responsibilities	Required Skills
Aerodynamics	• Airfoil Selection • Shaping & Sizing of Aerodynamic Bodies & Control Surfaces • Conducting Aerodynamic Simulations & Analyses for Efficiency, Stability, & Control	• Knowledge of Aerodynamics, Stability, & Aircraft Performance • Proficiency in Simulation & Analysis Software such as ANSYS and XFLR5 • Proficiency in CAD Software
Structure	• Designing, Modeling, & Selecting Materials for the Aircraft Structures • Conducting Physical & Analytical Structural Analyses of Components • Manufacturing Prototypes	• Knowledge of Material Properties, Structural Analysis, & Manufacturing Methods • Proficiency in CAD and FEA Software • Excellent Craftsmanship
Electronics and Propulsion	• Motor, Propeller Battery, & ESC Selection • Propulsion Sizing, Analysis, & Testing	• Knowledge of Propulsion Systems & Electronics • Ability to Conduct Static & Dynamic Thrust Tests
Budget	• Handling the Budget, Sponsorships, & Fundraising	• Excellent Budget & Communication Skills
Documentation	• Project Documentation, Including the Development of Detailed Charts, Figures, & Concise Written Segments	• Excellent Technical Writing & Organization Skills • Proficiency in Graphic Design

then reviews the schedule and determines which tasks should be done and in what order. The team meets weekly, and each subteam presents the work that has been done throughout the week. This ensures that each subteam is aware of design developments from other subteams. Open conversation about design decisions is encouraged to ensure all factors

are taken into consideration for each part of the design. When a conflict arises between the considerations of two teams, the team lead ensures that a compromise that satisfies both teams is found.

2.2 Schedule

At the start of the design process, the team made a chart of all the milestones and important dates needed for the competition. The chart follows the team's progress up until the competition. To stay organized, all tasks and deadlines were uploaded into Jira software along with the Gantt chart. This helped the team keep track of each task and who they were assigned to. The Gantt chart in Figure 2 shows the team's schedule from August 2023 up to the competition date in April 2024.
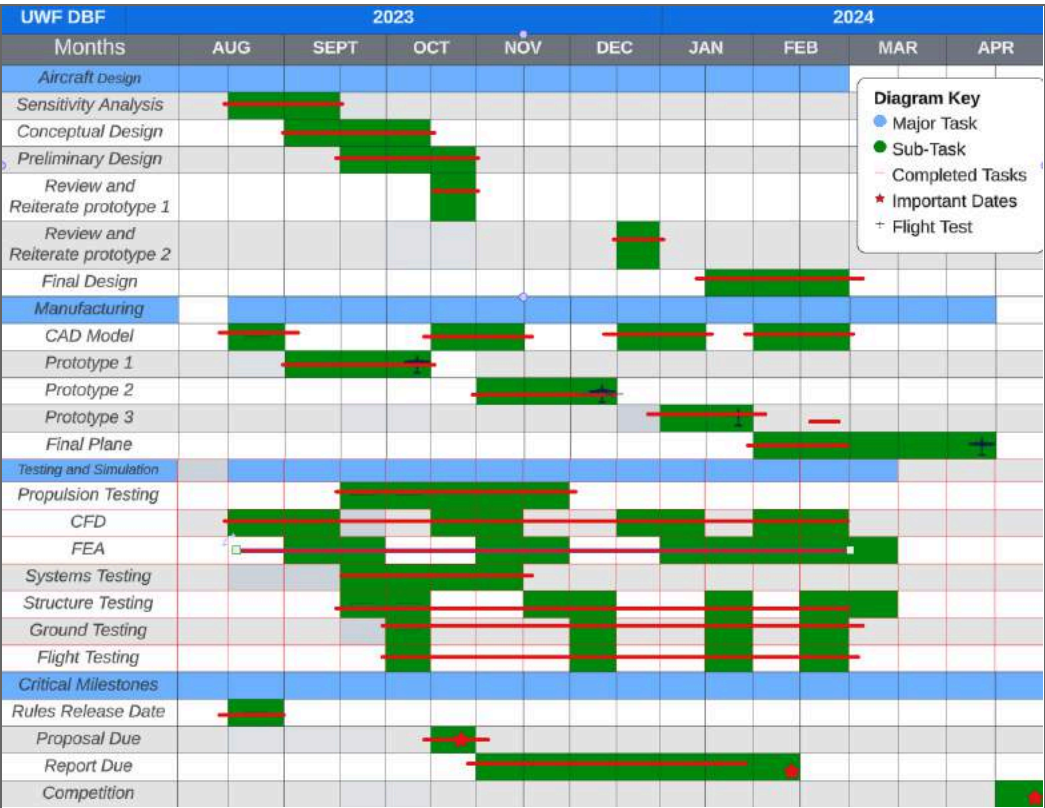
Figure 2: Gantt Chart

3. Conceptual Design

The conceptual design phase is to analyze the different mission requirements in order to adequately understand the design limitations. This involves an in depth scoring analysis of each mission equation to determine the best variables to optimize based on the scoring equations.

3.1 Mission Requirements

This year, the missions focus on urban air mobility. At competition, this will include demonstrating a flight around the circuit with no payload other than the crew, then simulating an air ambulance with the EMTs, passenger on a gurney, and a medical supply cabinet, and finally simulating a commercial

Figure 3: Course Layout [1]

flight with a payload of passenger dolls. The aircraft will have 20 feet to take off after the starting line of the course, shown in Figure 3, and will complete at least 3 laps per flight mission. All of the wooden dolls needed for the payload will be

provided at the competition. The crew, EMTs, and passengers will be represented by a 3.5 inch tall doll, which is shown in Figure 4, and the patient will be represented by a 5.5 inch doll like the one in Figure 5.

Mission 1: Plane Delivery Flight

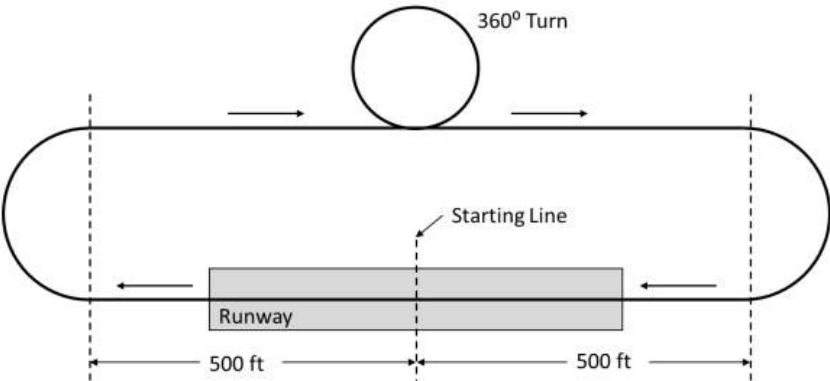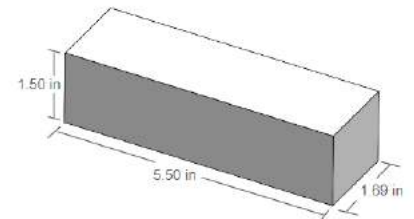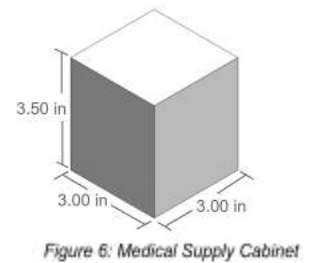The first flight mission will be flown with the crew only. The aircraft must first enter the staging box in its parking configuration. Then, the ground crew will reconfigure the aircraft into its flight configuration and install the batteries and Crew within 5 minutes. The aircraft must then take off within 20 feet and complete 3 laps within a 5-minute flight window. A lap is considered complete once the aircraft passes over the start/finish line in the air. If the aircraft makes a successful landing, the flight will be rewarded with a fixed score of 1.0 points.

Figure 4: Crew, EMT, and Passenger Doll [1]   Figure 5: Patient Doll [1]
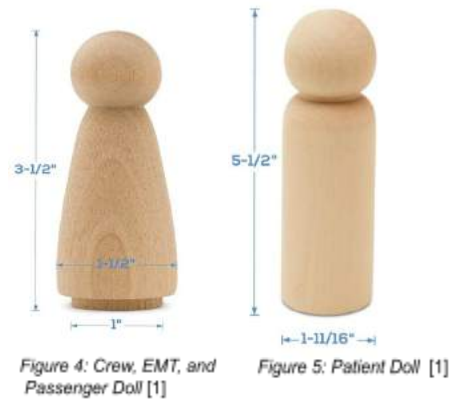
Mission 2: Medical Transport Flight

For the second flight, the aircraft will simulate an air ambulance by carrying the Crew, EMTs, the Patient on a gurney, and the Medical Supply Cabinet. The minimum dimensions for the Medical Supply Cabinet and the gurney are shown in Figures 6 and 7. Before the flight, the Medical Supply Cabinet will be weighed by the staging box judge while the aircraft is in its parking configuration. Then the ground crew will reconfigure the aircraft and load the entire payload and batteries within 5 minutes. The aircraft's goal for this mission is to complete 3 timed laps as fast as possible under a 5-minute flight window. The time will start once the throttle is advanced for take-off and will end once the aircraft passes over the start/finish line in the air after the final lap. The flight score will be a function of both payload weight and flight time.

Figure 6: Medical Supply Cabinet

Figure 7: Patient Gurney

Mission 3: Urban Taxi Flight

The final flight mission will be flown with the crew and passengers. This time, the battery capacity and number of passengers will be recorded by the staging box judge and afterward, the crew will have 5 minutes to transform the aircraft into its flight configuration and load the batteries and payload dolls. The goal for this flight is to utilize speed to fly as many laps as possible within the 5-minute flight window. Given a successful landing, the flight score will be a function of the number of laps flown, the number of passengers carried, and battery capacity.

Ground Mission: Operational Demonstration

The ground mission can be attempted at any time, with the goal being a quick demonstration of the aircraft's reconfiguration process for Missions 2 and 3. Since the score is based on mission time, time will start and pause each time the judge says "GO" and "STOP." After each pause, the judge will verify that all hatches are closed and secured and that all flight controls are operating properly. The aircraft will begin the mission in its parking configuration with no payload or batteries. Once cued, the crew member will put the aircraft into its flight configuration, load and secure the payload for Mission 2, and secure all of the hatches. When the time restarts, the crew member will switch out the payloads for

Missions 2 and 3 and secure everything once again. For the final stage, the crew member will unload Mission 3's payload, reconfigure the aircraft into its parking configuration, and place it in the parking spot. Once completed, the total mission time will be recorded.

3.2 Design Requirements Based on Mission Requirements

Beyond the mission requirements, the aircraft must satisfy and comply with the general design criteria and restrictions outlined in the rules. These are summarized in Table 2.

Table 2. General Requirements

Category	Requirement
General	• The Aircraft must not be a rotary or lighter-than-air configuration
Avionics & Propulsion	• Must use only one battery pack per propulsion system • Must use either NiCad/NiMH or lithium batteries • Must use a separate battery for the servos • Batteries cannot exceed 100 Watt-Hours • The ESC's BEC must be disabled • Must have an externally accessible radio-control switch • The arming fuse current rating cannot exceed 100 amps • Must be propeller-driven and electric-powered • May only use commercially produced propellers/blades • May only use unmodified commercial electric motors
Aerodynamics	• Must withstand 2.5G wingtip loading test • Wingspan must be less than 5 feet in length
Structure	• There must be a solid bulkhead behind the crew • The passenger compartment hatch cannot extend past the fuselage vertical centerline • Hatched must be less than 6 inches wide • The crew must be loaded via a separate hatch • The crew's heads must be positioned above the nose • The passenger compartment must have a single plane, horizontal floor • The aircraft must be configured to fit into a 2.5-foot-wide parking space without removing any components
Payload	• The payload dolls must have a restraint system • The patient must be secured to the gurney • The payload dolls cannot touch each other • The crew must consist of a pilot and a co-pilot • The EMTs must be alongside the patient
Takeoff	• Must use ground rolling takeoff • Must takeoff within 20 feet of the starting line • All energy for takeoff must come from on-board propulsion battery pack(s) • TOGW must be less than 55 lbs

Each mission's requirements are shown in Table 3. To ensure that the mission requirements could be met, the team broke down the requirements into a list of design objectives for the propulsion, aerodynamics, and structure sub-systems. These are outlined in Table 4 below.

Table 3. Mission Requirements

Mission		Mission Requirements
General Flight Requirements (GR)	GR.1	Takeoff within 20 feet
	GR.2	Complete a successful landing
Mission 1 (M1)	M1.1	Carry the crew
	M1.2	Complete 3 laps under 5 minutes
Mission 2 (M2)	M2.1	Carry the crew, EMTs, patient on the gurney, and the Medical Supply Cabinet
	M2.2	Complete 3 laps as fast as possible
Mission 3 (M3)	M3.1	Carry the crew and passengers
	M3.2	Complete as many laps as possible within 5 min
Ground Mission (GM)	GM.1	Fit the aircraft into a 2.5-foot-wide parking space
	GM.2	Reconfigure the aircraft as quickly as possible
	GM.3	Load and unload the payload as quickly as possible

Table 4. Subsystem Requirements

Sub-System	Mission	Sub-System Requirements
Propulsion	M1.2, M3.2	Has an endurance of at least 5 min
	GR.1	Has sufficient thrust for short takeoff capability
	GR.1, M2.2, M3.2	Has high efficiency for maximum speed and minimum power usage
Aerodynamics	GR.1, M2.2, M3.2	Minimizes surface area to lower drag and maximize speed
	GR.1, M2.1, M3.1	Generates sufficient lift for all flight configurations
	M1.2, M2.2, M3.2	Has high stability and control to withstand high-g maneuvers
Structure	GM.1	Can be reconfigured to a width less than 2.5 ft
	GM.2	Has an efficient reconfiguration process
	GM.3	Has an easily accessible payload
	M1.1, M2.1, M3.1	Has sufficient volume for the crew and passenger compartments
	GR.2, M1.1, M2.1, M3.1	All major components have sufficient strength to withstand maximum loads
Payload	M2.1, M3.1, GM.3	Has optimized configurations for payload storage
	GM.3	Has a simplistic restraint system

3.3 Scoring Analysis

The team analyzed the scoring equations for each mission very early in our design process. The team created summaries of each mission to ensure every team member could easily understand what was required of our plane. The summary and scoring equations were used to break down each mission into specific sub-system requirements. Table 5 provides a succinct summary of the mission, scoring equation and sub-system requirements for each mission.

Table 5. Mission Scoring Equations and Subsystem Requirements

Mission	Summary	Score Equation	Sub-system Requirements
Mission 1 (M1)	Complete 3 laps within 5 minutes with Crew only	$M1 = 1.0$	Plane must takeoff, fly three laps, and land successfully without payload
Mission 2 (M2)	Carry a medical supply cabinet, patient, EMTs and crew for three timed laps	$M2 = 1 + \dfrac{\left(\frac{Payload\ Weight}{Time}\right)_N}{\left(\frac{Payload\ Weight}{Time}\right)_{Max}}$	Score will increase with a higher payload weight and a lower three lap time
Mission 3 (M3)	Complete as many laps as possible in 5 minutes while carrying passengers as payload	$M3 = 2 + \dfrac{\left(\frac{\#\ laps\ *\ \#\ passengers}{Battery\ Capacity}\right)_N}{\left(\frac{\#\ laps\ *\ \#\ passengers}{Battery\ Capacity}\right)_{Max}}$	Score will increase with a higher number of laps completed in 5 minutes, higher number of passengers carried, and lower battery capacity
Ground Mission (GM)	Change between mission configurations while timed	$GM = \dfrac{(Mission\ Time)_{Min}}{(Mission\ Time)_N}$	Score will increase with lower time to change between configurations

Using the scoring equations for each mission, the team conducted scoring sensitivity analyses in Excel and MATLAB [2]. Specifically, sensitivity analyses for Missions 2 and 3 were created, as well as the Final Score. Score for Mission 1 is a constant 1 or 0 points provided, based on completion or failure of the missions, respectively. Once the plane is capable of completing this mission, nothing more can be done to increase the score for this mission through altering the plane's design. Missions 2 and 3 are the missions for which the score will vary based on the plane's performance during flight. Therefore, those were focused on most during the sensitivity analyses. The factors that will impact score in Mission 2 are time for three laps and payload weight carried. The variables affecting Mission 3 score are number of laps in five minutes, number of passengers carried, and battery capacity. When analyzing variation of total score in Excel, the team chose the payload weight capacity, time per lap, and battery capacity as our variables. These were used in the Mission 2, Mission 3 and Final Score sensitivity analyses. The scoring sensitivity plots in Excel for Mission 2 score, Mission 3 score, and the final score can be found in Figures 8, 9, and 10, respectively.
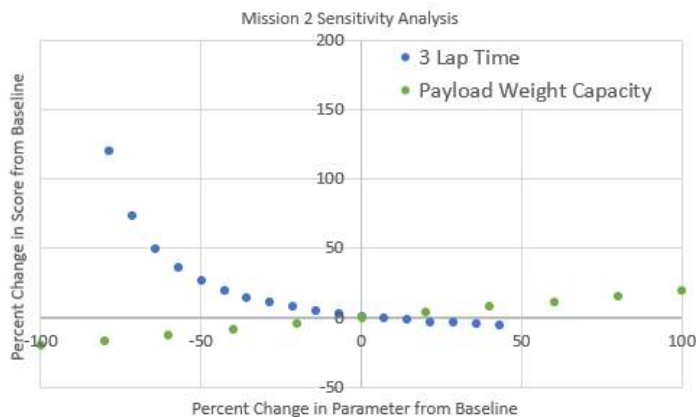
Figure 8. Mission 2 Score Sensitivity Analysis
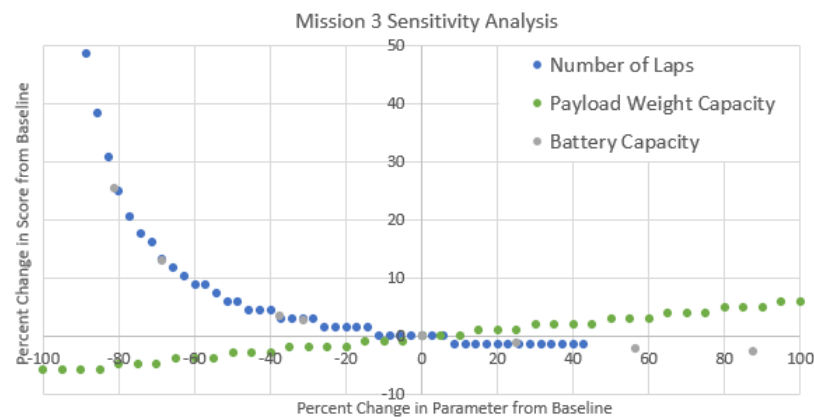
Figure 9. Mission 3 Score Sensitivity Analysis
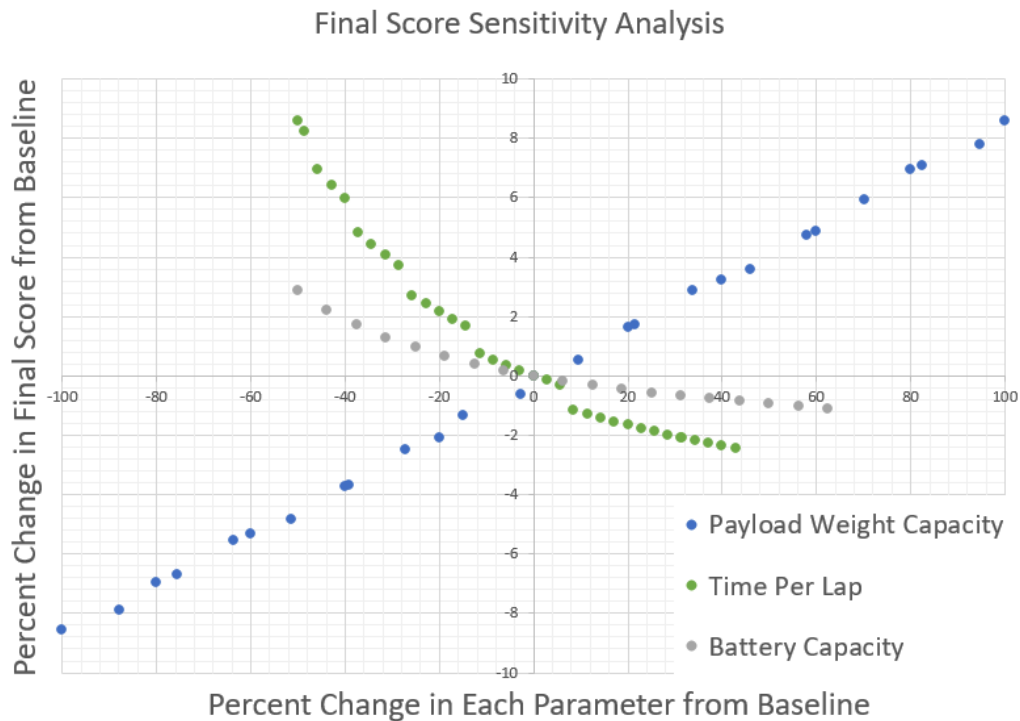
Figure 10. Final Score Sensitivity Analysis

One trend the team noticed is that Mission 2 is dependent upon continuous variables, while Mission 3 is dependent upon discrete variables. In the sensitivity analysis for the Final Score, the overall score is inversely proportional to time per lap and battery capacity, and is proportional to payload weight capacity. The team concluded that our score would be best served by creating a plane primarily built for reducing time per lap and battery capacity while carrying a modest payload. If we decide to design the plane to carry more payload, our ground mission score could also suffer. The effect of more passengers on the ground mission score will be determined through a series of timed drills meant to simulate the ground mission at competition. A 3D MATLAB plot of Final Score vs Payload Weight and Time per Lap, shown in Figure 11, was also created to visualize the effect varying these parameters would have on the final score. The continuous and discrete nature of Mission 2 and 3's variables, respectively, can also be seen in the 3D scoring analysis.
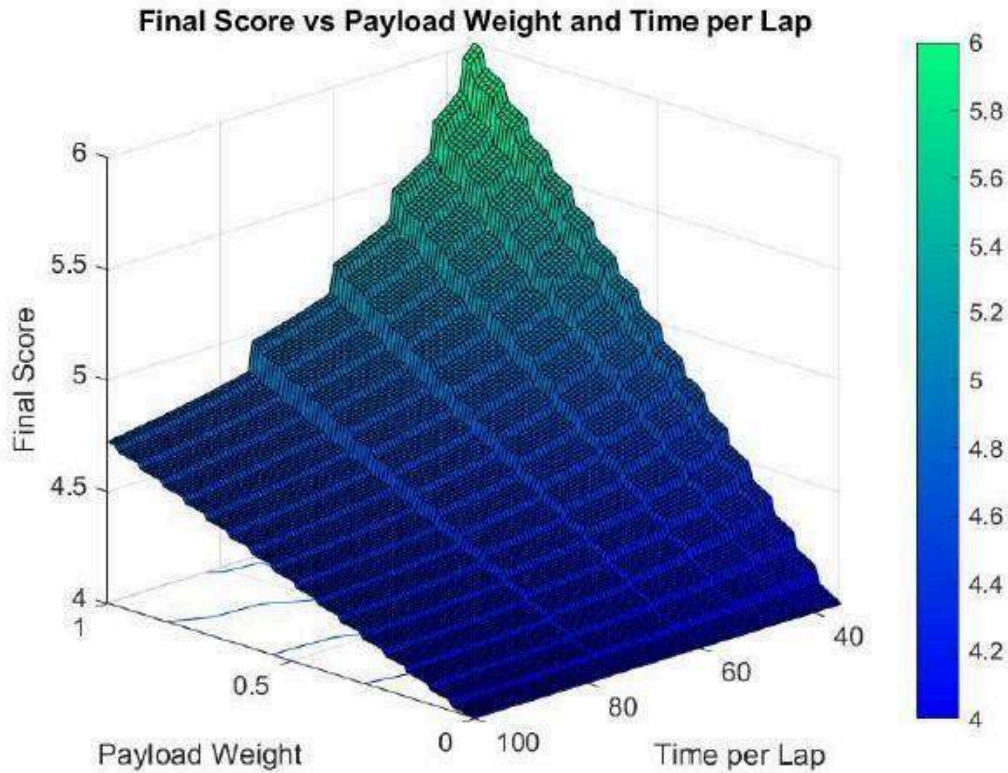
Figure 11. MATLAB 3D Plot of Final Score against Payload Weight and Time Per Lap

Based on the scoring analyses, the main mission parameter to focus on for Missions 2 and 3 is decreasing lap time. The secondary goal is to maximize payload weight for Mission 2 and the number of passengers for Mission 3. Mission 2's payload is in the form of a medical supply cabinet of our chosen weight concentrated in one location. Mission 3's payload will be multiple passengers distributed throughout the fuselage, which must remain secure during flight. Mission 3's score will also increase as the onboard battery capacity decreases.

Feedback from the proposal indicated that the team should convert the trends found in the scoring sensitivity analysis into aircraft design parameters. One equation that can be used to analyze the aircraft design parameters that will affect payload weight is the takeoff distance equation (1).

$$s_{LO} = \frac{1.44\,W^2}{g\rho_\infty S C_{L,max}\,T}$$

(1)

By solving this equation for weight, the team found that for a given takeoff distance, weight (and therefore payload) is proportional to the square root of wing area, max coefficient of lift, and static thrust. Wing area can be increased by increasing either the span or the chord of the wing. When increasing chord length, the team must be conscientious of the decrease in aspect ratio. A decrease in aspect ratio would increase lift-induced drag. Maximum wing lift coefficient could be increased through airfoil selection or the addition of flaps. Static thrust can be increased through motor-propeller combination selection, but this may necessitate using a larger battery, which would decrease score for Mission 3.

When considering optimizing our plane for a low time per lap, the team considered the forces of thrust and drag on a plane in straight and level flight. Propeller thrust decreases as freestream velocity increases, and drag force increases proportionally to the square of velocity. A velocity will be reached where thrust matches drag. The plane will spend a majority of Missions 2 and 3 at this velocity. Therefore, it is important to consider the design parameters that affect these forces when designing the plane. Thrust will be analyzed by using eCalc and dynamic thrust testing to characterize how thrust changes with freestream velocity. Drag force is found using equation (2).

$$D = \frac{1}{2}\rho V^2 S C_D$$
(2)

When designing a plane, the team can reduce the area or the drag coefficient of a body. Components exposed to the airflow, such as the fuselage and landing gear, should be designed to reduce drag coefficient. Drag created by a wing has two distinct components: lift-induced and parasite drag. A wing's coefficient of drag is given by equation (3).

$$C_D = C_{D,0} + \frac{C_L^2}{\pi e AR}$$
(3)

One major consideration when reducing a wing's coefficient of drag is airfoil selection. Because drag coefficient increases with the parasite drag coefficient and the square of the lift coefficient, an airfoil should be found that provides a low coefficient of drag and high lift-to-drag ratio. To reduce induced drag, the airfoil that provides the lowest coefficient of lift necessary for takeoff should be used. Efficiency factor, e, is a factor that compares a lift distribution to an ideal lift distribution (elliptical). This can be changed by changing the wing's planform shape. However, different planform shapes have different manufacturability and stall concerns, so these must be taken into consideration during the plane's design. Increasing aspect ratio can also reduce a wing's coefficient of drag.

3.4 Configurations Considered and Selection Process

The team considered three different aircraft configurations, including monoplane, biplane, and canard designs. A monoplane is the most simplistic design and the easiest to manufacture. It can support a higher payload capacity since it has less drag compared to a biplane and is considered to be more efficient. However, it has less maneuverability and requires higher wing loading. A biplane tends to have good lifting characteristics for a short wingspan and is capable of achieving short takeoffs and landings. Its higher roll rate and maneuverability would also make it easier to navigate the circuit. Yet having two wings would add manufacturing complexity and induce more drag, which would make the aircraft slower. This is undesirable as speed is a critical scoring factor for Missions 2 and 3. A canard was considered because it can help generate additional lift to complement the wing during takeoff and can offer more control authority. However, like the biplane, introducing an additional aerodynamic surface will induce more drag compared to a monoplane and the canard's downwash could interfere with the wing's performance. Furthermore, a canard configuration has higher complexity, as a canard is typically difficult to optimally size. Thus, given the sub-system requirements in Table 4, the team

decided that a monoplane configuration was the best option due to its design and manufacturing simplicity, higher payload capacity, and its ability to achieve higher speeds.

4. Preliminary Design

After choosing an aircraft configuration, the team was able to start conducting design and sizing trade studies. This process also involved analyzing components through software programs such as XFLR5 and ANSYS to predict performance and later on, using physical testing to verify results.

4.1 Design/analysis Methodology

The flowchart in Figure 12 shows the methodology for designing, analyzing, and manufacturing the final aircraft. The chart breaks up the main issues, where each box shown in the flowchart signifies an assignment for a specific subgroup to find a solution and share with the group. The main analysis method for the team to analytically determine a component is viable to be placed on the final plane. Then test the component separately and if it fails go back to the design and sizing portion of the flowchart. Repeat this process to slowly improve the overall design.
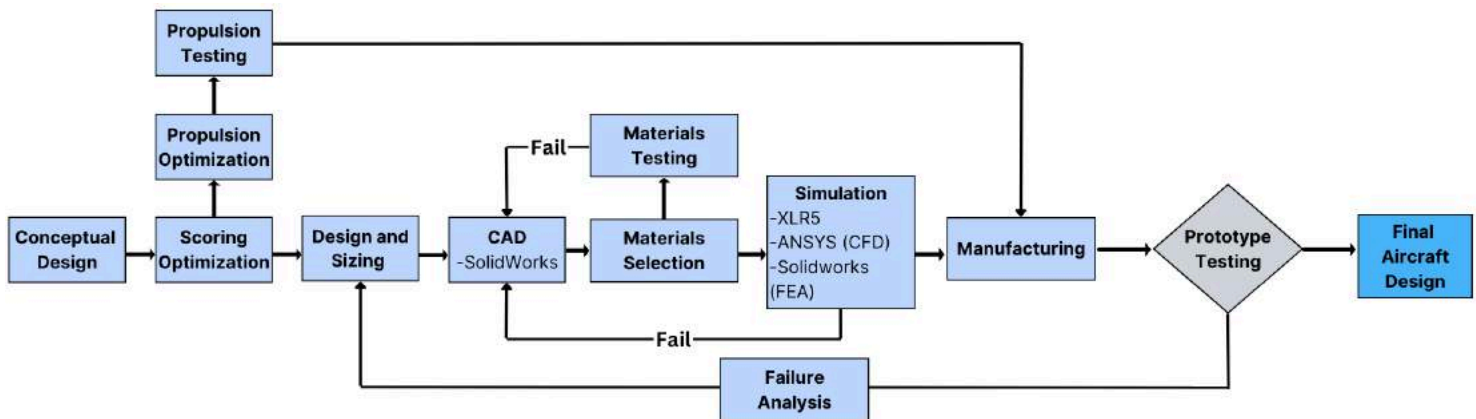
Figure 12. Design and Build Process Flowchart

4.2 Design and Sizing Trades

The team followed an iterative process to develop the aircraft's preliminary design. The goal was to develop a high performing aircraft that satisfied all of the mission requirements and could achieve the highest score possible based on the key results outlined in the scoring analysis. The design adapted as new findings and observations from trade studies, analyses, and physical tests were made for each component. For testing, the team had to consider the fact that Wichita has a slightly lower air density and more extreme wind conditions than Pensacola, as both of these environmental conditions had the potential to impact predictions for flight performance. Given that the competition will take place in Spring while most of the team's testing will be completed during Winter, Table 6 provides a summary of the environmental differences between the competition's airfield in Wichita and the team's test field in Pensacola.

Table 6. Condition Comparison of Wichita and Pensacola

Condition	Wichita, KS	Pensacola, FL
Season	Spring	Winter
Avg. Temp ($^{\circ}$F)	57	57
Avg. Wing (mph)	19.1	9.8
Elevation (ft)	1385	50
Air Density (lb/ft^3)	0.07688	0.077136

4.2.1 Preliminary Fuselage Shape and Sizing

To minimize the aircraft's weight and drag characteristics, the preliminary fuselage was sized around the minimum dimensions required to house the payload dolls and medical supply cabinet in Missions 2 and 3, resulting in a maximum 4 x 6-inch filleted rectangular cross-section. For the crew member section, the top of the main fuselage was shaped to slope downward to create a "window," and a space for a top hatch, so that the 2 crew members would have a clear line of sight over the nose while situated on a floor insert. In front of the crew, the nose was sized as a small 4 x 4 inch cross-section to house the avionics, with the battery extending below the crew dolls to reduce surface area further. The back of the fuselage was shaped to taper down completely to form a flat bottom surface, which made the total fuselage length 40 inches. The length of the main payload compartment was based on estimating the maximum number of passengers the aircraft could hold for Mission 3 and the minimum length required to house the payload for Mission 2. A summary of the preliminary fuselage sizing, which was modeled in Prototypes 2 and 3, is shown in Figure 13 below. The initial design was simplified to make prototyping with foam poster board an easier process.
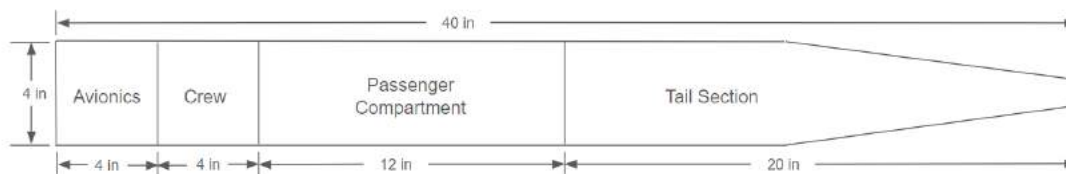
Figure 13. Drawing of Preliminary Fuselage Shape and Sizing

Since the fuselage's structure must have sufficient strength to accommodate all of the required loads, the team had to decide on whether it would be worth continuing to use foam board for the fuselage's structural material or if it would be beneficial to switch to a stronger material like balsa wood or carbon fiber. Foam board was used for prototyping because it is a lightweight material, is easy to work with, and is forgiving in most incidents. However, prior competitions have

demonstrated that it has poor structural integrity under high loading and given the mission requirements, it would not be a desirable choice. The team also considered balsa wood because it has a higher strength than foam and is low in density. The main concern however, was that balsa can fracture easily and in the event of a crash, especially given the harsher environmental conditions in Wichita, the aircraft would most likely be rendered unusable afterward due to a lack of repairability. Ultimately, the team decided that carbon fiber, despite its high manufacturing complexity, would be the best choice for the fuselage's structural material since it poses less risk for structural failure due to its high specific strength. With a monocoque structure, the carbon fiber skin will be the major load-bearing component.

Since speed was considered a critical factor for Missions 2 and 3, a fuselage shape trade study was later conducted to minimize the fuselage's drag coefficient from the team's preliminary model by performing CFD analyses in ANSYS Fluent [3] at a speed of 50 miles per hour. Opting to use carbon fiber also provided more leeway for developing a more streamlined fuselage shape since negative 3D-printed molds could be utilized for manufacturing. The focus of this study was mainly on the shape and length of the fuselage's aft section. Initially, some consideration was given to utilizing a single-tail boom design as it could help decrease weight. However, testing eventually showed that this would induce too much turbulent airflow and drag compared to a continuous fuselage-tail extension, and would also add more manufacturing complexity. Therefore, the team chose to remain with a conventional configuration.

When comparing taper configurations, such as a high taper to the top surface of the fuselage like Prototype 1, a low taper like Prototypes 2 and 3, and a mid-plane taper, there was not a significant difference in drag coefficient values found. However, a clear pattern emerged that out of the configurations, a low taper had the most drag, followed by the high taper, and then the mid-plane taper. Concerns regarding wing downwash affecting the performance of the horizontal stabilizers ultimately influenced the team to go with a high-tapered aft section given a low-wing configuration.

To create a smooth transition from the rectangular passenger compartment to the empennage, the aft section was shaped to taper vertically along a gentle curve to the top surface, and all of the fuselage edges were filleted. The overall fuselage length was also extended to 48 in from the preliminary design since this would provide better stability characteristics given the aircraft's wing size. Figure 14 is the pressure coefficient plot along the length of the fuselage with the nose starting on the left side. It shows low variation in pressure at the aft tail section, which indicates that the boundary layer remains attached. As a result of streamlining, the fuselage's drag coefficient ended up dropping from 0.104, for the preliminary design of Prototype 3, to 0.025. Figure 15 shows the simulations performed in ANSYS Fluent [3].
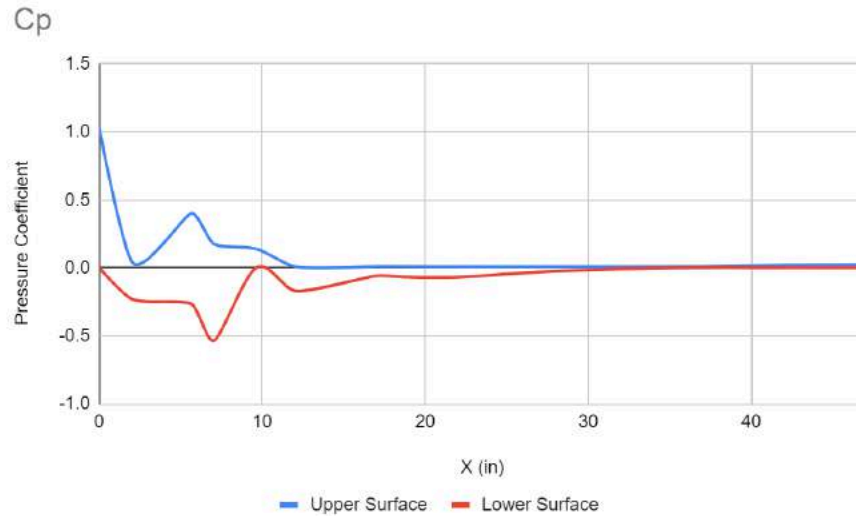
Figure 14. Plot of Pressure Coefficient for Fuselage
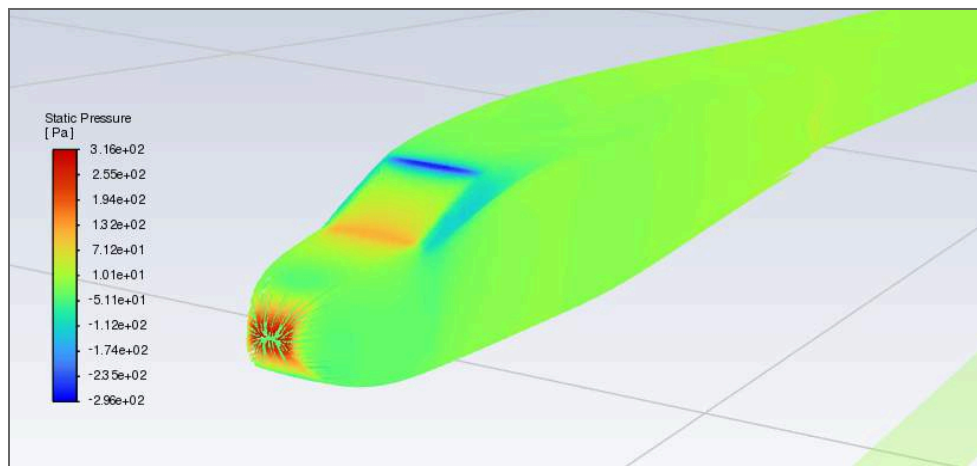
Figure 15. Ansys Fluent Fuselage Simulation

4.2.2 Preliminary Parking Configuration Design

Three major designs were considered for meeting the requirement of the plane being able to fit within a 2.5 foot parking space. The 1st major design was to fold the wing on a hinge point on each wing. The 2nd was a rotating wing while parked. The 3rd design was folding the fuselage in half and having the back fuselage hinge and sit on top of the front of the fuselage.

Folding Wing Design

Initially, a folding wing design was considered to fulfill the 2.5 foot parking space requirement. A folding wing design allows for a monocoque or semi-monocoque fuselage design requiring very little internal framing when used in conjunction with high strength composite materials like fiberglass or carbon fiber. A folding wing

Figure 16. Folding Wing Concept Example

16

design also moves the folding mechanism weight out onto the wings, helping with load distribution, potentially allowing for an overall lighter weight design when compared to other folding mechanisms. Despite these performance benefits, it was ultimately decided that moving the folding mechanism onto the wings brought too much mechanical and manufacturing complexity to the design.

Rotating Wing Design[1]

A rotating wing design was briefly considered to meet the 2.5 foot parking space requirement. This design was inspired by NASA's AD-1 oblique wing aircraft design. However, instead of rotating the wing in flight for improved aerodynamic performance, the wing would only be rotated on the ground to be as close to parallel with the fuselage as possible. This would allow for a mechanically simple, single spar wing design to be used in conjunction with a monocoque or

semi-monocoque fuselage. Ultimately, this design was not fully developed due to the complexity of the landing gear required to produce this wing design in a low-wing configuration. Although a high-wing rotating design would not conflict with landing gear, the drawbacks of a high wing configuration outweighed the advantages of the rotating wing design.

Figure 17. AD-1 Oblique Wing

Folding Tail Design

Several designs for a folding tail were considered, and were ultimately narrowed down to two candidates. A folding tail design would allow for the parked length of the aircraft to be approximately halved to fit in the 2.5 foot parking space requirement with a fixed monoplane design. Implementing a folding tail design instead of a folding wing design would allow for easier design and manufacturing of the wing and cabin assembly. The reduced complexity of the wing design would result in a reduced overall weight because the wings could be supported structurally with a single, solid wing spar.
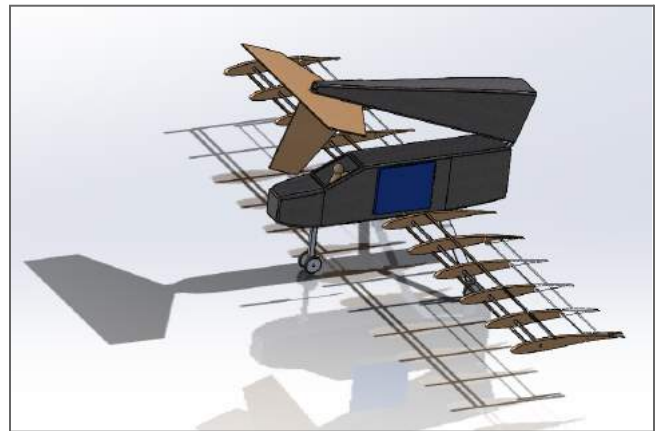
Figure 18. Folding Tail Concept Example

Candidate 1: Simple Hinge and Latch Design

The original idea for a folding fuselage design was to simply have a wide hinge at the top of the break in the fuselage and a latch on the bottom. This design would be very easy to manufacture and relatively lightweight. This version of a folding fuselage would have some challenging drawbacks to overcome, namely lateral stability of the empennage. With only a connecting structure on the top and bottom of the fuselage, rudder inputs would result in a torque about the hinge that

---

[1] AD-1 Photo Courtesy of NASA https://www.nasa.gov/reference/ad-1/

may not be adequately stabilized. This would result in unwanted flex in the fuselage potentially resulting in poor handling characteristics or even structural failure. Additionally, making the rotation axis of the hinge perpendicular to the centerline of the fuselage would result in limited rotation because the tail would interfere with the cockpit assembly when folded. Ultimately, a slight variation of the simple hinge and latch design was chosen. To address the horizontal flexing concern, an overlapping bracket design was implemented on the sides of the fuselage that slide into rails on the empennage. The finalized design of the simple hinge was the simplest to produce and lightest weight based on rough estimates of parts required for each design.

Candidate 2: Offset Hinge and Dowel Design

This design was created to address the shortcomings of the simple hinge design. To address the structural concerns, a pin and dowel system would be implemented at the attachment point between the main fuselage and empennage. Curved dowels would allow for a standard hinge to be used, however, curved dowels would be both difficult to manufacture and difficult to slide in operation. Therefore, a linear sliding mechanism would be attached to the hinge to allow the dowels to first be disengaged before the empennage is folded. Additionally, the hinge is mounted at a shallow angle to the fuselage centerline. This would allow the vertical stabilizer to be folded next to the cockpit without interfering with the rest of the fuselage.
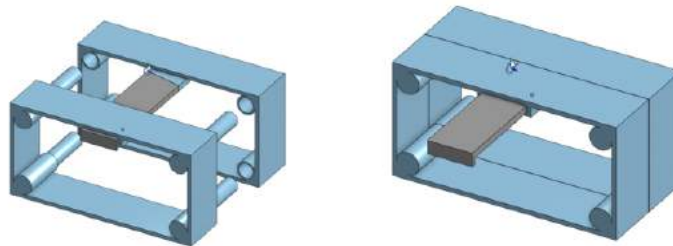
Figure 19. Offset Hinge and Dowel Concept

4.2.3 Preliminary Passenger Design and Sizing

The preliminary design for passenger configuration and sizing was first copied from the DBF rules and made as a Solidworks template as shown in Figure 20, which represents Mission 2's payload. Using the template was a good starting point for spacing and estimating the size of the fuselage's payload compartment. Since the crew has to enter their compartment through a separate hatch from the rest of the payload, the template was split into two. The crew will drop into and rest atop of their insert before being loaded through a top hatch on the fuselage. For Mission 2, the Medical Supply Cabinet and patient will be loaded through a 6-inch wide hatch on the side of the fuselage. Due to the size constraint of the hatch, the Medical Supply Cabinet will be loaded first and pushed to the far side of the payload compartment to make room for the patient and EMTs. For Mission 3, the payload compartment will house only passenger dolls, which will be able to fit through the hatch on an insert 6 at a time in 2 rows of 3 sitting side-by-side. The team estimated the maximum number of passengers that could be carried by
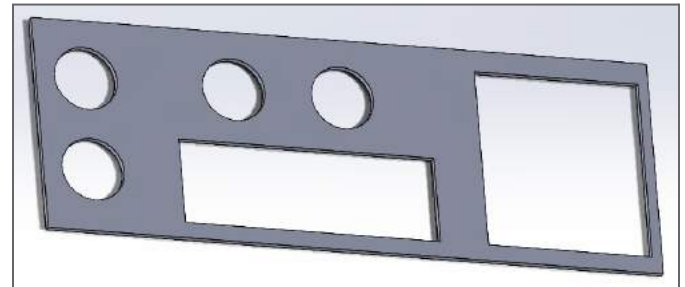
Figure 20. Preliminary Passenger and Design Configuration

the aircraft to be 12. For security, the payload dolls will be strapped with velcro.

4.2.4 Preliminary Landing Gear Design

The advantages and disadvantages of different configurations of landing gear were discussed. The trade study was based on the landing gear's ability to taxi, take off, land, and drag. The configuration of tricycle landing gear was chosen mainly due to the ease of takeoff and landing. To negate the ground loop as much as possible, tricycle landing gear is the best. The pros and cons can be seen in Table 7.

Table 7. Landing Gear Configuration Comparison

4.2.5 Preliminary Wing Design and Sizing

4.2.5.1 Airfoil Selection

The team used airfoiltools.com to research and download potentially useful airfoils [4]. The team analyzed characteristics at a Reynolds number of 200k, as our simulations indicated the operating Reynolds number during takeoff for our plane trended towards that. For the team to be awarded a score, it is imperative that the team meets the takeoff distance limitation of 20 feet. The team initially selected 7 airfoils, which included the AG10, Eppler 176, FX 60-100, NACA6412, FX76-MP-120, S1210, and S1223 airfoils. Because the team is optimizing our plane to be lightweight and fast, the team decided to analyze airfoils with a wide range of coefficients of lift. Airfoil data was obtained through XFLR5 [5]. Plots of coefficient of lift against angle of attack are shown for the chosen airfoils in Figure 21. A higher coefficient of lift value will increase the induced component of drag for the plane, so the team would like to use the airfoil with a modest coefficient of lift. Ideally, the airfoil's coefficient of lift will be as small as possible while still allowing for takeoff within the 20 feet limitation. The ideal airfoil for our design would also have a low coefficient of drag, as well as a high lift-to-drag ratio. These characteristics were plotted in Figure 22 and 23, respectively. An airfoil that has consistent performance at low Reynolds numbers would also be preferred, as this would reduce the chance of poor performance during takeoff and

landing. The chosen airfoil must also have space for an adequate structure and be easy to work with from a manufacturing perspective.
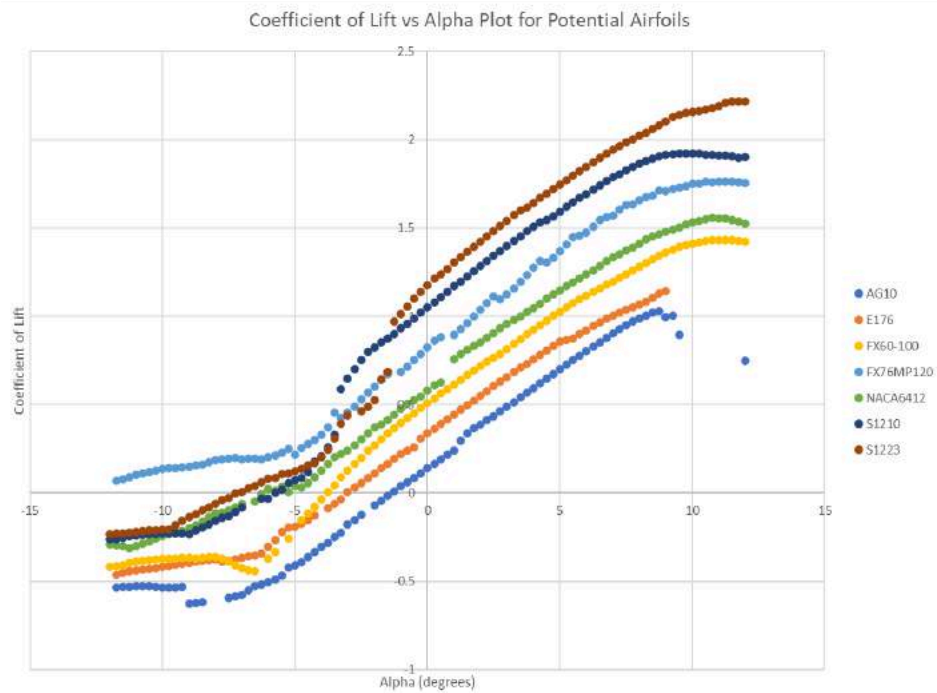
Figure 21. Plot of Coefficient of Lift Against Angle of Attack for Chosen Airfoils
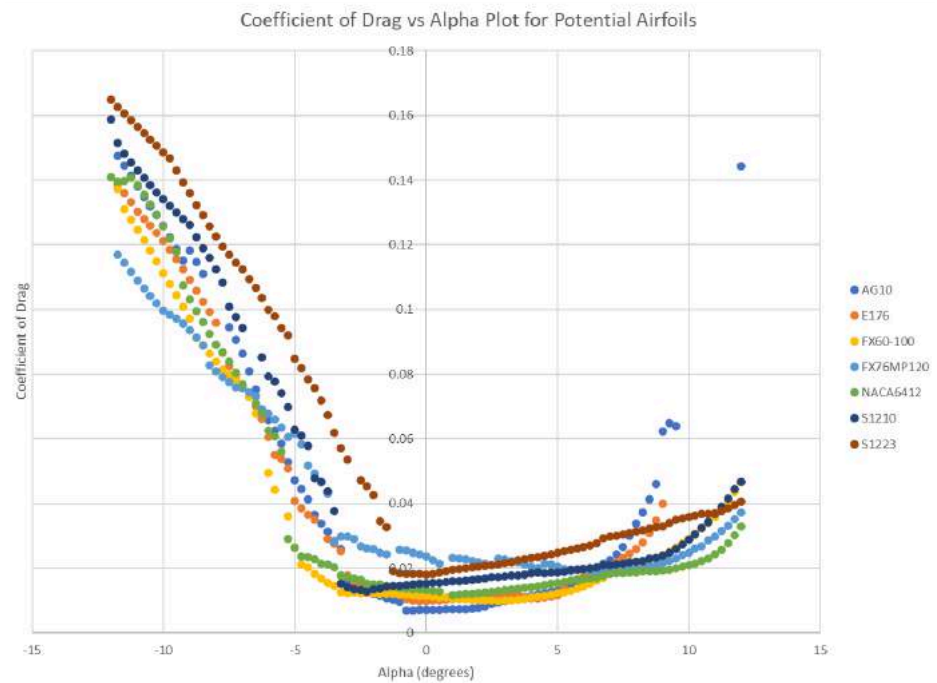
Figure 22. Plot of Coefficient of Drag Against Angle of Attack for Chosen Airfoils

20
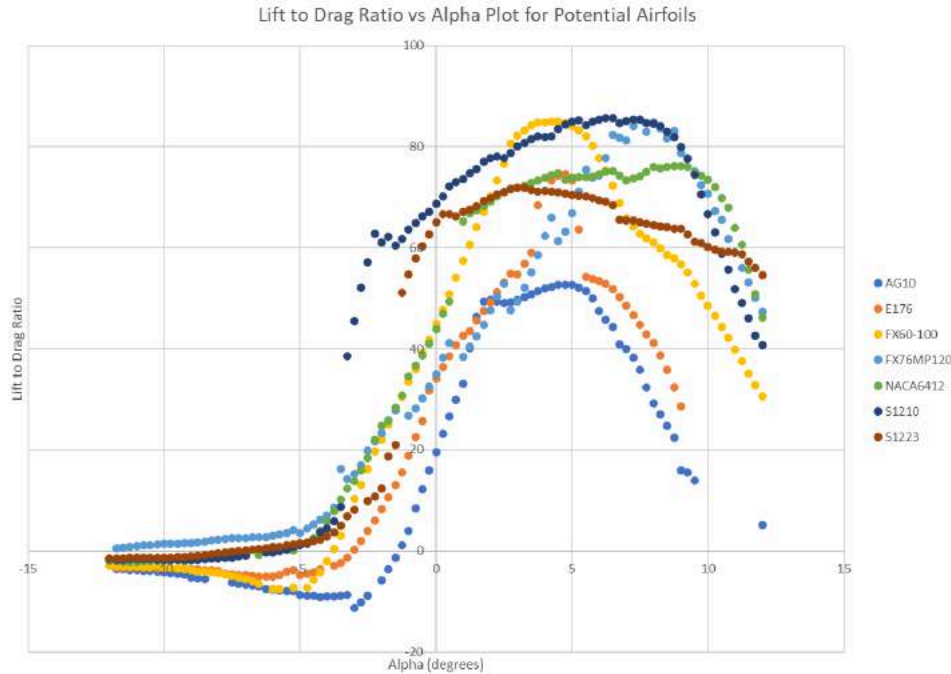
Figure 23. Plot of Lift-to-Drag Ratio Against Angle of Attack for Chosen Airfoils

The team compared the maximum lift coefficient, minimum drag coefficient, and maximum lift-to-drag ratio of each airfoil. These characteristics form the quantifiable portion of our overall airfoil comparison and are shown in Table 8. Two qualitative factors, performance at low Reynolds number and manufacturability, were considered later in the process.

Table 8. Lift and Drag Characteristics for Selected Airfoils

Airfoil	Maximum Coefficient of Lift (α, degrees)	Minimum Coefficient of Drag (α, degrees)	Maximum Lift-to-Drag Ratio (α, degrees)
AG10	1.0080 (8.50)	0.00697 (-0.75)	52.67 (4.75)
Eppler 176	1.2403 (10.75)	0.00912 (-1.25)	74.57 (4.75)
FX 60-100	1.4470 (12.25)	0.00981 (2.75)	84.92 (4.50)
NACA6412	1.5895 (10.75)	0.01120 (0.50)	76.21 (9.00)
FX76-MP-120	1.7335 (11.50)	0.01816 (6.50)	85.45 (7.50)
S1210	1.9628 (14.50)	0.01233 (-2.75)	85.41 (7.25)
S1223	2.2919 (13.00)	0.01758 (-0.25)	71.91 (3.25)

The team used the takeoff distance equation to approximate the amount of weight a wing constructed from each airfoil could carry. With an estimated plane weight of 5 pounds, any budgeted weight in excess of 5 pounds could be allotted for

21

carrying payload. Alternatively, a chord length decrease or wing taper would be viable if the airfoil coefficient of lift was high enough. These would serve to increase aspect ratio and Oswald efficiency factor, which will reduce induced drag. However, reducing chord length could present problems in the higher lift airfoils. The higher lift airfoils in our selection had poor performance at low Reynolds numbers, the most egregious example of this being the S1223 airfoil. Each airfoil's performance at Reynolds numbers between 20k and 200k was compared, with performance characterized as "Good", "Medium" or "Poor". These were color coded, as can be seen in Figures 24 and 25 and weighted accordingly. If chord length were decreased, the characteristic length and therefore Reynolds number of our wing would decrease, making poor performance more likely. The FX 60-100 airfoil had mostly consistent performance for a 20k-200k range of Reynolds number, which would serve to improve performance at lower speed. The FX 60-100 airfoil's shape provides adequate space for a wing structure. The dramatic changes in thickness present throughout the S1223 airfoil, for example, could make the placement of adequate structure difficult. Having a larger chord length also ensures space for adequate structure within the wing ribs. These factors were combined into manufacturability considerations in our overall airfoil comparison.
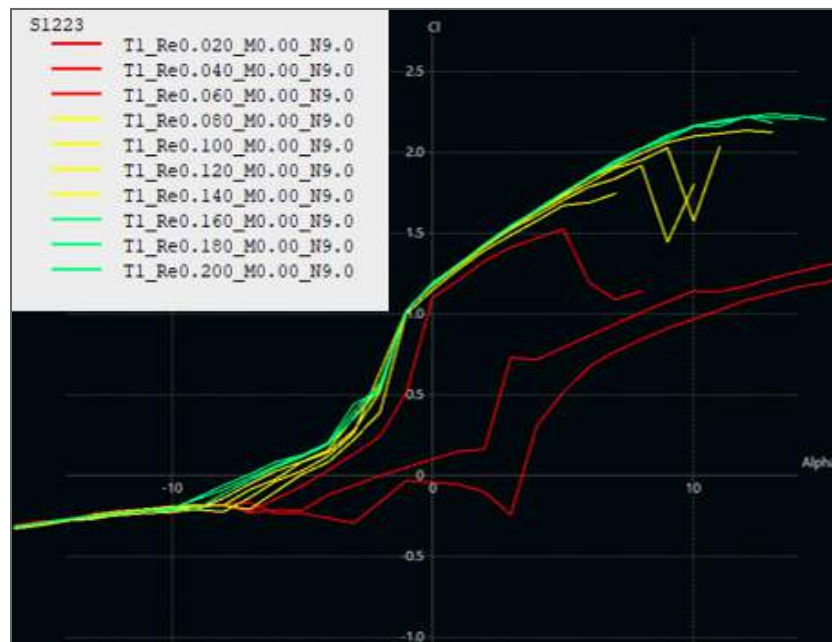
Figure 24. S1223 Airfoil Performance at Low Reynolds Number Values
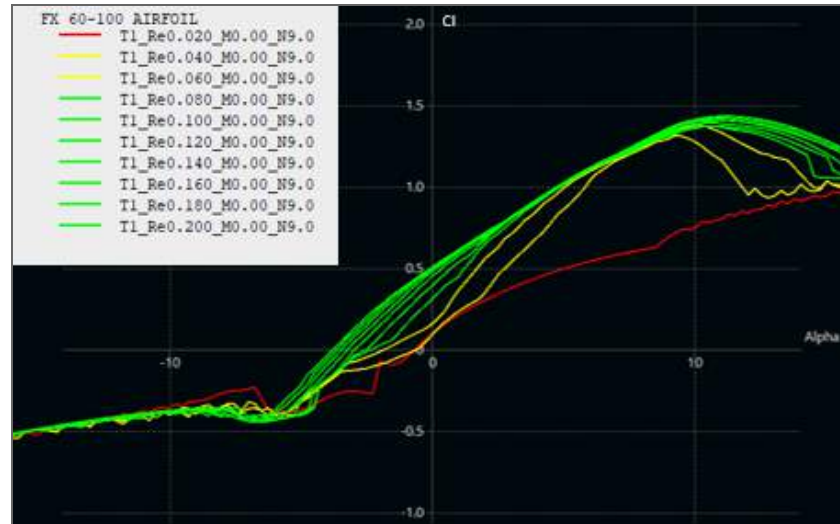
Figure 25. FX 60-100 Airfoil Performance at Low Reynolds Number Values

The team compared the quantifiable factors (maximum lift coefficient, maximum drag coefficient, and maximum lift-to-drag ratio) by weighting them as a fraction of the best performer in that category. Examples of the weighting of performance at low Reynolds number can be seen above. Manufacturability was assigned based on reviewing the airfoil shapes. The average of the airfoil's performance in each column was used as the total score when comparing airfoils. A graphic representation of these comparisons is shown in Table 9 below.

Table 9. Weighted Overall Airfoil Comparison

Airfoil	Maximum Lift Coefficient Weighted	Minimum Drag Coefficient Weighted	Maximum Lift-to-Drag Ratio Weighted	Low Reynolds Number Performance Weighted	Manufacturability Weighted	Overall
AG10	0.4398	1.0000	0.6164	1	0.1	0.6312
Eppler 176	0.5412	0.8816	0.8727	0.9	0.7	0.7791
FX 60-100	**0.6314**	**0.8436**	**0.9938**	**0.9**	**0.6**	**0.7938**
NACA6412	0.6935	0.7671	0.8919	0.55	0.8	0.7405
FX76-MP-120	0.7564	0.3838	1.0000	0.3	0.5	0.5880
S1210	0.8564	0.7048	0.9995	0.7	0.3	0.7122
S1223	1.0000	0.4157	0.8415	0.4	0.2	0.5715

According to our comparisons, the FX 60-100 airfoil had the best overall performance and was therefore chosen for the design and construction of our wing.

4.2.5.2 Wing Planform Shape and Sizing

One aspect of the wing that required a trade study was the wing planform shape. The team considered rectangular, elliptical, and tapered planform shapes for our wing. Aerodynamic efficiency, stall characteristics and ease of manufacturing were considered when comparing the planform shapes. An increase in aerodynamic efficiency will result in a reduction in drag according to the equation for the coefficient of induced drag for a wing. Increasing aerodynamic efficiency will therefore serve to decrease our time per lap, which would increase our score. A wing that has poor stall characteristics will be difficult to control at low speeds, increasing the risk of a crash during takeoff and landing. If a crash occurs at competition, the team could lose valuable flight attempts due to the time it would take to make repairs. This leads to the third tradeoff when considering planform shape: manufacturability. The rectangular planform would be the easiest to design, manufacture and repair, as each rib would have the same dimensions. Previous wing designs created based on a tapered planform shape were extremely difficult to create in SolidWorks. When considering manufacturing and repairability, the team would need replacement ribs for each length of chord present in the ribs. Additionally, the team has experience applying Ultracote to wings that utilize a rectangular planform, but never a tapered or elliptical planform. A tapered or elliptical planform could cause construction difficulties to arise. These factors were compared according to table 11.

Table 11. Planform Comparison

Planform	Efficiency	Stall Characteristics	Manufacturability	Overall
Rectangular	0.8	1	1	0.933
Tapered	0.9	0.8	0.8	0.833
Elliptical	1	0.8	0.6	0.8

With the wing and fuselage dimensions decided, the team was able to begin sizing of the horizontal and vertical stabilizers. The team sized the stabilizers by using the non-dimensional volume ratio equations (Equations 4 and 5 below) [6].

$$C_{HT} = \frac{S_{HT} \cdot L_{HT}}{S_W \cdot c_{MAC}} \quad (4) \qquad C_{VT} = \frac{S_{VT} \cdot L_{VT}}{S_W \cdot b} \quad (5)$$

The team used Raymer's volume coefficients for Civil Homebuilt props (Cht = 0.500 and Cvt = 0.040) to find the required horizontal and vertical stabilizer areas [6]. Next, some stabilizer aspect ratio guidelines were used to further define the horizontal and vertical stabilizer dimensions. According to a guideline for the horizontal tail, the aspect ratio of the horizontal tail should be less than the wing aspect ratio. This ensures that the horizontal stabilizer will not stall before the wing, and the plane will retain pitch authority despite a wing stall. The recommended value of aspect ratio for a vertical stabilizer is 1.3-2.0. Finally, the team will implement a taper ratio of 0.5 on both stabilizers. This will ensure the forces on the stabilizers will be concentrated closer to the fuselage, reducing the structural load at the tip of the stabilizers.

Table 10. High Wing and Low Wing Comparison

High Wing	Low Wing
+ More ground clearance for taxi/takeoff- easier to maneuver.	- Less ground clearance- small obstacles present a challenge.
* Reduced ground effect- longer takeoff, but shorter landing rolls.	* Stronger ground effect- shorter takeoff, but longer landing rolls.
- Inherently stable- center of mass is below center of lift, requiring less dihedral and easier to handle as a remote pilot. This also has the effect of making the aircraft effectively lower performance, which is not desirable for the shortest possible lap time.	+ Inherently unstable- center of mass is above center of lift, requires excess dihedral or more skilled pilot to remain in S/L flight. In this case,
+ Better crosswind handling- due to shallower required dihedral, crosswinds have significantly less effect on aircraft handling.	- Poorer crosswind handling- due to steeper dihedral, crosswinds tend to roll the aircraft, requiring more aileron input.
- Structurally complex- often requires a wing spar to help evenly distribute weight and landing gear is more complex/heavier.	+ Simpler structure- a shared main spar simultaneously supports fuselage, wing, and landing gear.
- More difficult to configure- due to the small nature of the aircraft, a high wing impedes reconfiguring of the cabin between missions. (Typically, opposite on full-scale aircraft)	+ Better access to cabin- this makes reconfiguring the aircraft between missions easier for an R/C plane. (Typically, opposite on full-scale aircraft)
- More difficult to fold- a folding wing mechanism would be significantly more difficult to implement, partially due to previously mentioned non-ideal load distribution throughout the plane's structure.	+ Easier to fold- implementing a folding mechanism is easier due to the shared load bearing spar. This allows for minimal weight gain from a folding mechanism.
+ Less impact from gear configuration- fixed vs retractable gear has insignificant impact on wing performance.	- Greater impact from gear configuration- fixed gear significantly reduces wing performance compared to retractable gear.
- More susceptible to damage- in the event of a crash, the wings absorb little force often resulting in a higher structure failure rate.	+ Distributed crash forces- in the event of a crash, the wing contacts the ground at the same time as the fuselage, sometimes resulting in less structural damage.

For the position of the wing on the aircraft a high wing configuration was chosen initially for its greater stability and better landing performance. However, it was found that the initial prototype was not agile enough to maneuver through the course in an efficient manner and it was determined that bracing structures like wing struts would be necessary on the final design. Therefore, a low wing configuration was chosen for its ease of manufacturing, better cabin accessibility, greater ground effect, simple shared main structural wing spar, and inherent instability. All of these aspects of a low wing configuration combined allows for the optimal balance of simplicity and performance to be achieved.

4.2.6 Preliminary Avionic and propulsion Design and Sizing

The preliminary avionics design is the research and development of the electronics of the aircraft. The research and development determined the final electronics design and ensured the safety of the aircraft in flight.

4.2.6.1 Propulsion Battery Optimization

Due to the scoring equation for Mission 3, the plane's main propulsion battery will need the lowest milli-amp hours for the maximum score. A lower milli-amp commercially viable battery is a 3200mAh spectrum battery. Through calculations to determine the power draw needed and the minimum amount of battery amp hours in Excel, it was determined that the best combination was a 3200 mAh battery and a motor that draws 38 amps or less. A combination of a 2200 mAh battery was tested, however, the highest the motor draw could be for the battery to last 5.06 minutes is 26 amps. The reason the 3200 mAh battery was chosen is due to the motor torque and thrust output at this amperage. The motor torque at this amperage will be able to produce 2000g of static thrust which is sufficient for a takeoff distance of less than 20 feet.

$$Maximum\ battery\ Life = \frac{Battery\ Capacity\ (mAh)}{Load\ Current\ (A)} = \frac{3200}{38000} = 0.084\ hrs * \frac{60\ min}{1\ hr} = 5.05\ min \quad (6)$$

4.2.6.2 Receiver Battery Optimization

The small battery powers the receiver and servos. Due to there being no restrictions on battery capacity, the team chose to go with a higher factor of safety battery that has more battery capacity than needed. The absolute minimum amount of time to power the battery is 5.5 minutes because the majority of flights are only allowed to have a flight time of 5 min per the DBF rules. The servos used to control the control surfaces are spectrum A500 servos. The servos were chosen due to the calculations performed to find the maximum amount the torque needed to deflect oncoming air shown on equation 7 and 8. Each spectrum A500 servo draws 1.2A at max deflection. By multiplying the stall amperage draw of the spectrum servo by the number of servos used within the aircraft a total load current can be calculated. The stall amperage of the spectrum A500 is 1.2 A. Equation 7 shows the maximum current draw of 6 servos. Equation 8 shows the maximum battery life of a 1000mAh battery that is being used by the 6 servos.

$$Total\ Current\ Load = (Servo\ stall\ amperage) * (number\ of\ servos) = 1.2A * 6 = 7.2A \quad (7)$$

$$Maximum\ battery\ Life = \frac{Battery\ Capacity\ (mAh)}{Load\ Current\ (A)} = \frac{2000}{7200} = 0.276\ hrs * \frac{60\ min}{1\ hr} = 16.66\ min \quad (8)$$

4.2.6.3 Motor and Propeller

Due to the 38 Amp maximum current the motor can draw based on the sizing of the 3200 mAh Spektrum battery. The search for a motor is limited to motors that draw less than 38 Amps to ensure the plane flies for the 5-minute mission duration time. eCalc [7] was used to find the best matches of motor and propeller combinations that draw less than 38 Amps. The choice came down to 2 motors, the Cobra 3515/14 kv 950 and the Flysky 2826C V2 Kv 720 motors. Both motors utilize a single tractor configuration on the plane. Testing occurred through static and dynamic thrust tests.

4.2.6.4 Electronics

The electronic speed controller being used for the aircraft is a 50A controller. The draw from the motor will reach a maximum amperage of 39A. To ensure no failure would occur due to over-drawing the ESC, an ESC with a maximum amperage of 10 more than what the motor will draw was chosen. The ESC chosen is an E-flite 50 AMP Brushless ESC.

Table 12. Variables Used in Torque Calculations for Servo Sizing

Parameters	Value
Aileron Length (in) (L)	22
Aileron Chord (in) (C)	0.1016
Speed (mph) (V)	22
Max Control Surface Deflection (degrees)	15
Max Servo Deflection Angle (degrees)	15
Air Density (kg/m^3)	1.204
Drag Coefficient (Cd)	1.28
Lift Coefficient (Cl)	0.033
Torque (lb*ft)	**0.204**

For the preliminary designs the plane uses a total of 4 servos that actuate the two ailerons, rudder, and elevator. The equations used in Figure 26 solve for the minimum torque requirement for servos [8]. To determine the correct sized servo for the final plane, the maximum torque needed based on the control surfaces area and maximum airspeed needed to be determined. To find the maximum speed of the plane, the propulsion system is examined. The motor and propeller combination has a maximum wind speed of 50 miles per hour according to eCalc [7]. The data for servo specification can be found in Table 12. The servos being selected need to have a torque rating of 0.204 lb*ft or higher. The servos selected to be used for both aileron control surfaces is the Spektrum A6380 servos. The manufacturer's rated torque for the A6380 is 0.832 lb*ft. The other servos being used are Spektrum A500 that will be used to control the rudder and elevator. The torque rating for the A500 servo is 0.152 lb*ft. The free body diagram shown in Figure 26 shows the forces working on a servo [9].

Where:
C: Control surface chord (in)
L : Control surface length (in)
A : Control surface Area (in^2) = Control surface chord * Control surface length
V : Speed (mph)
C_D: Drag Coefficient
C_L: Lift Coefficient
θ : Maximum deflection angle of the   control surface (degree)
θ1:Maximum deflection angle of the servo (degree)
r : The distance from pivot point to the force F (m)
ρ : Air density 1.293 kg/m3

$$\Sigma M(Pivot\ Point)\ =\ (\tfrac{-C}{2}sin\theta)(-F_{drag}) + (-r)(F)(cos\theta 1) + (-\tfrac{-C}{2}cos\theta)(-F_{Lift}) \quad (9)$$

To find the maximum torque the equation shown below is used.

$$\tau\ =\ cos(\theta 1)[(\tfrac{-C}{2}sin\theta)(-\tfrac{1}{2}\rho C_d V^2 C_L) + (-\tfrac{-C}{2}cos\theta)(-\tfrac{1}{2}\rho C_L V^2 C_L)] \quad (10)$$

Figure 26. Torque Calculations for Servo Sizing

Figure 27 shows the circuit diagram between the electrical components. The plane's electrical system consists of 1 3200 mAh battery to power the propulsion system. A 2000 mAh battery to power the 6 servos and receiver. A red arming fuse to break the connection of propulsion and a switch to turn the receiver off. The large battery is connected to the 50 Amp ESC (electronic speed controller) which is connected to the receiver.
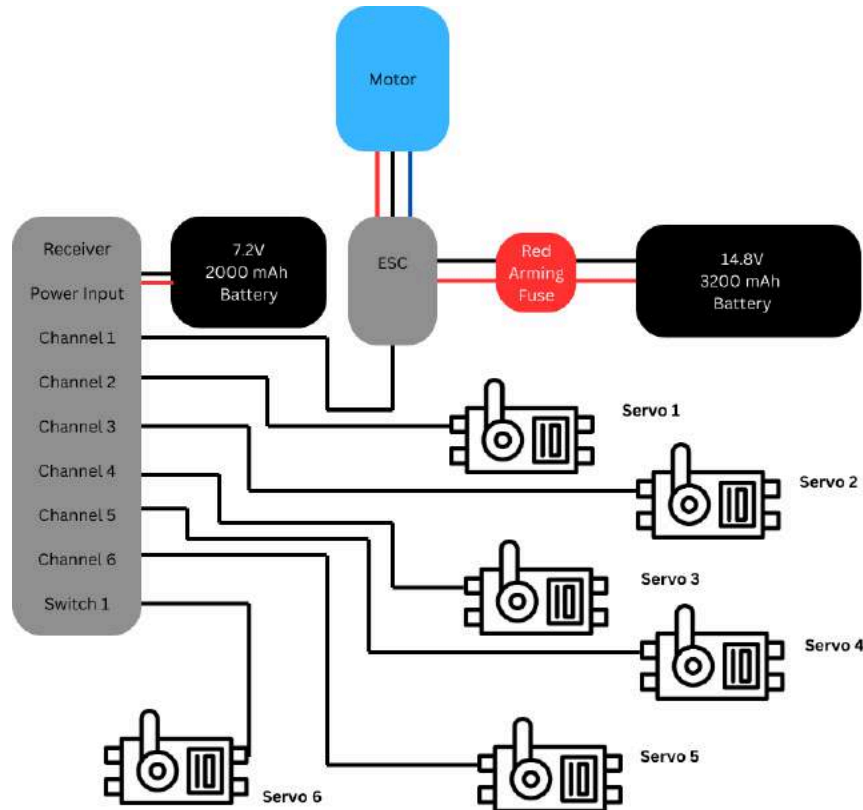
Figure 27. Wiring Diagram

4.3 Aircraft Performance Prediction

The performance of our proposed design was evaluated using multiple simulation software. The team created simulations of plane performance in Excel and MATLAB. The team combined the knowledge gained in Dynamics, Numerical Methods, and Dynamic Systems to create our simulations. The simulations utilize the plane's equations of motion, based primarily on the four fundamental forces of flight, in the X and Z direction. The acceleration in each direction is found by dividing the sum of forces in that direction by the mass. This acceleration is then "integrated" to velocity using a numerical method. The dependence of the thrust, lift, and drag forces on velocity is accounted for in our simulations. The velocity in each direction is then "integrated" to position. The team has modeled plane performance in prior competitions this way using

Excel, so creating another performance simulation in Excel was easy. Feedback from prior competitions indicated that while the simulation was a good idea, our use of Euler's Method could have affected the accuracy of our simulation. The team decided to create simulations using higher order methods. The team created flight performance simulations utilizing the 4th Order Runge-Kutta numerical method to "integrate" acceleration to velocity, then velocity to position. One simulation was focused on the plane's performance during takeoff. The results of this simulation approximately matched the takeoff distance calculations. The plane lifted off at 16.2 feet along the runway and is shown in Figure 28.
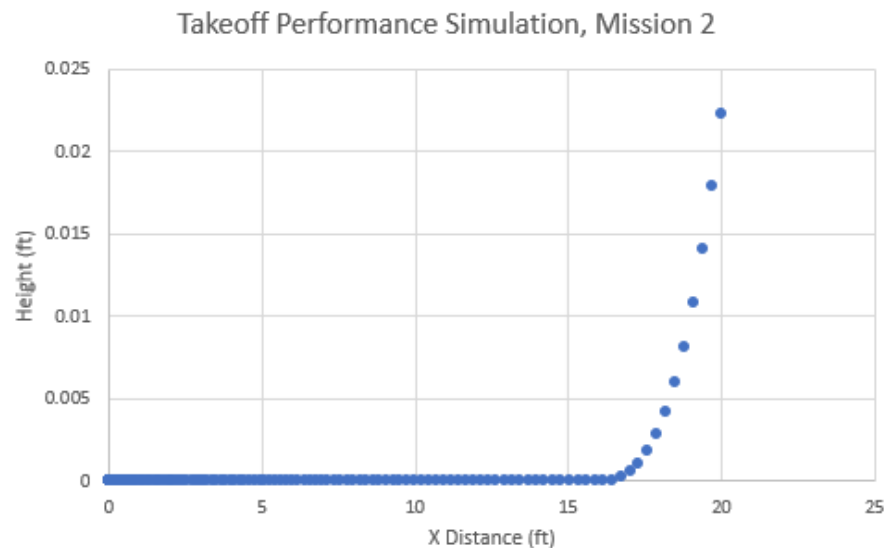

Figure 28. Takeoff Performance Simulation for Mission 2

The MATLAB simulation was created using the Simulink Blockset. Simulink Blockset allows for the use of integrator blocks, allowing for higher order numerical methods to be used with ease. Simulink automatically chooses a method based on the situation and defaulted to a third order numerical method (ode3, Bogacki-Shampine). The simulation provided takeoff predictions that matched prototype and Excel simulation performance. The plane began to take off at 15.6 feet according to the Simulink simulation.

4.4 Lift, Drag, and Stability Characteristics

4.4.1 Lift

The wing must provide adequate lift to allow for takeoff within the 20 feet allotted by the competition. A rectangular planform wing that utilizes the FX 60-100 airfoil was the chosen final design. The adequacy of potential wing designs for takeoff was verified using both the takeoff distance equation and plane performance simulations utilizing numerical methods. Wing lift characteristics were obtained using XFLR5 [5].

4.4.2 Drag

Another Runge-Kutta Excel simulation was created to solve for the plane's cruise speed. While the takeoff distance simulation accounted for the forces in the X and Z direction, this simulation was constricted to thrust and drag. The coefficient of drag for our plane was found by summing the coefficient of drag of individual plane components. The team recognizes that this may be an underestimate due to interference drag between combined components, but the division of

29

individual components among different subteams made summing the individual components the most viable option. Balanced flight occurs in the X direction when thrust matches drag. Thrust decreases proportionally with airspeed, and drag increases proportional to the square of velocity. Thrust and drag were plotted against velocity, which can be seen in Figure 29 to find where the forces in the X direction balance.
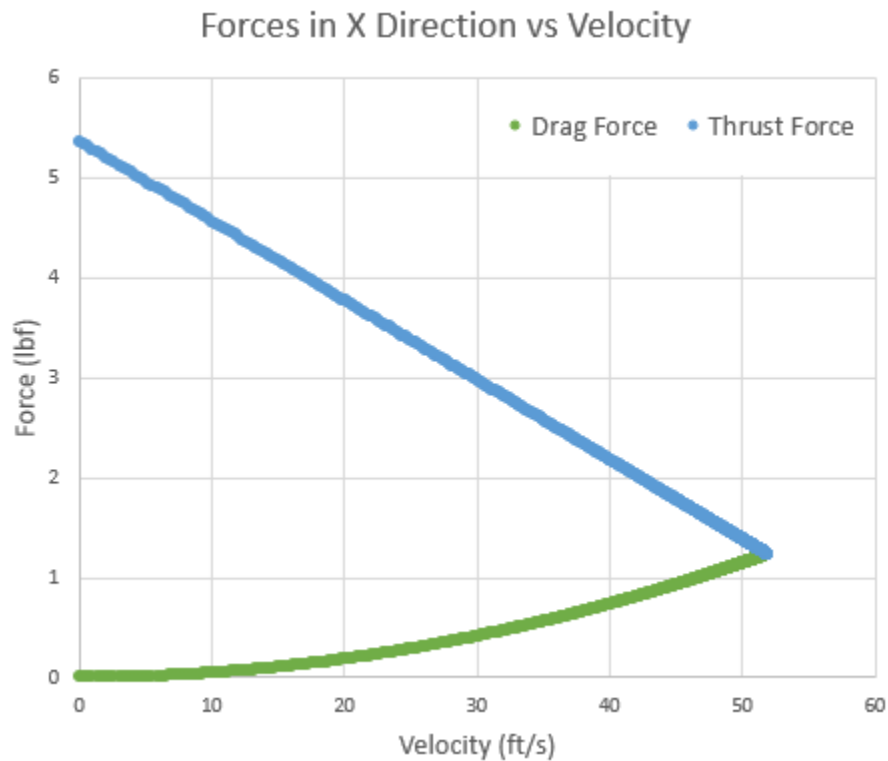

Figure 29. Plot of Thrust and Drag Force vs Velocity

Thrust and drag were found to balance at an airspeed of 51.9 feet per second. This airspeed will create an approximate single lap time of 38.54 seconds.

4.4.3 Stability

The team used the weight and balance tables (shown in the Detail Design section, as dictated by the Scoring Rubric) of the plane extensively when analyzing the stability of our design. XFLR5 was also used for our wing and horizontal stabilizer's coefficients of lift and location of center of pressure. The team analyzed static stability by solving for static margin as a percentage of the mean aerodynamic chord. An airplane is considered to be statically stable if the restoring moments return the plane to its trim condition [10]. Static margin represents the distance between the neutral point and the center of gravity. The sign convention the team used for weight and balance involved treating distances from the nose tip towards the empennage as positive, so positive static margin will be defined as being aft of the center of gravity. The team used XFLR5 to find the coefficients of lift for the wing and horizontal stabilizer at varying angles of attack, as well as the distance of the wing's center of pressure from the wing's leading edge. The team then found the lift from the stabilizer and wing at our predicted airspeed. The sum of these lift forces and the sum of their moments about the nose tip was then

found. Dividing the sum of moments from the lift forces about the nose tip by the sum of lift forces provided the distance of the neutral point from the nose tip. The distance of the center of mass from the nose tip was then subtracted from the distance of the neutral point from the nose tip. This value was divided by the mean aerodynamic chord to provide a dimensionless value of the static margin at varying angles of attack. This was repeated for all three flight missions. According to our sign convention, a positive static margin will provide a nose down moment and a negative static margin will provide a nose up moment. The results of these calculations can be seen in Tables 13, 14 and 15.

Table 13. Calculations for Static Margin at Varying Angles of Attack, Mission 1

Angle of Attack (degrees)	Wing Lift Coefficient	Lift from Wing (lbf)	Location of Center of Pressure (ft)	Horizontal Stabilizer Coefficient of Lift	Lift from Horizontal Stabilizer (lbf)	Sum of Lift Forces (lbf)	Sum of Moment (lbf*ft)	Location of Neutral Point (ft)	Static Margin
-5	0.4156	1.8451	1.3653	-0.3543	-1.5728	0.2722	-3.7723	-13.8569	-15.0198
-4	0.4935	2.1909	1.3502	-0.2468	-1.0956	1.0953	-1.4243	-1.3004	-2.4634
-3	0.5686	2.5241	1.3392	-0.1627	-0.7221	1.8020	0.4919	0.2730	-0.8900
-2	0.6404	2.8427	1.3305	-0.1000	-0.4440	2.3986	2.0060	0.8363	-0.3266
-1	0.7127	3.1638	1.3237	-0.0493	-0.2189	2.9448	3.3121	1.1247	-0.0382
0	0.7872	3.4944	1.3184	0.0004	0.0016	3.4960	4.6133	1.3196	0.1567
1	0.8598	3.8167	1.3140	0.0500	0.2221	4.0388	5.9037	1.4617	0.2988
2	0.9312	4.1340	1.3102	0.1008	0.4475	4.5815	7.2064	1.5729	0.4100
3	0.9985	4.4325	1.3069	0.1633	0.7249	5.1574	8.6923	1.6854	0.5225
4	1.0607	4.7086	1.3040	0.2477	1.0994	5.8080	10.5377	1.8143	0.6514
5	1.1217	4.9793	1.3013	0.3543	1.5729	6.5522	12.7711	1.9491	0.7862
6	1.1823	5.2485	1.2989	0.4545	2.0175	7.2660	14.8871	2.0489	0.8859
7	1.2383	5.4973	1.2965	0.5162	2.2916	7.7889	16.2937	2.0919	0.9290

Table 14. Calculations for Static Margin at Varying Angles of Attack, Mission 2

Angle of Attack (degrees)	Wing Lift Coefficient	Lift from Wing (lbf)	Location of Center of Pressure (ft)	Horizontal Stabilizer Coefficient of Lift	Lift from Horizontal Stabilizer (lbf)	Sum of Lift Forces (lbf)	Sum of Moment (lbf*ft)	Location of Neutral Point (ft)	Static Margin
-5	0.4156	1.8451	0.1653	-0.3543	-1.5728	0.2722	-3.7723	-13.8569	-15.0781
-4	0.4935	2.1909	0.1502	-0.2468	-1.0956	1.0953	-1.4243	-1.3004	-2.5216
-3	0.5686	2.5241	0.1392	-0.1627	-0.7221	1.8020	0.4919	0.2730	-0.9482
-2	0.6404	2.8427	0.1305	-0.1000	-0.4440	2.3986	2.0060	0.8363	-0.3849
-1	0.7127	3.1638	0.1237	-0.0493	-0.2189	2.9448	3.3121	1.1247	-0.0965
0	0.7872	3.4944	0.1184	0.0004	0.0016	3.4960	4.6133	1.3196	0.0984
1	0.8598	3.8167	0.1140	0.0500	0.2221	4.0388	5.9037	1.4617	0.2405
2	0.9312	4.1340	0.1102	0.1008	0.4475	4.5815	7.2064	1.5729	0.3517
3	0.9985	4.4325	0.1069	0.1633	0.7249	5.1574	8.6923	1.6854	0.4642
4	1.0607	4.7086	0.1040	0.2477	1.0994	5.8080	10.5377	1.8143	0.5931
5	1.1217	4.9793	0.1013	0.3543	1.5729	6.5522	12.7711	1.9491	0.7279
6	1.1823	5.2485	0.0989	0.4545	2.0175	7.2660	14.8871	2.0489	0.8277
7	1.2383	5.4973	0.0965	0.5162	2.2916	7.7889	16.2937	2.0919	0.8707

Table 15. Calculations for Static Margin at Varying Angles of Attack, Mission 3

Angle of Attack (degrees)	Wing Lift Coefficient	Lift from Wing (lbf)	Location of Center of Pressure (ft)	Horizontal Stabilizer Coefficient of Lift	Lift from Horizontal Stabilizer (lbf)	Sum of Lift Forces (lbf)	Sum of Moment (lbf*ft)	Location of Neutral Point (ft)	Static Margin
-5	0.4156	1.8451	0.1653	-0.3543	-1.5728	0.2722	-3.7723	-13.8569	-15.1000
-4	0.4935	2.1909	0.1502	-0.2468	-1.0956	1.0953	-1.4243	-1.3004	-2.5436
-3	0.5686	2.5241	0.1392	-0.1627	-0.7221	1.8020	0.4919	0.2730	-0.9702
-2	0.6404	2.8427	0.1305	-0.1000	-0.4440	2.3986	2.0060	0.8363	-0.4068
-1	0.7127	3.1638	0.1237	-0.0493	-0.2189	2.9448	3.3121	1.1247	-0.1184
0	0.7872	3.4944	0.1184	0.0004	0.0016	3.4960	4.6133	1.3196	0.0764
1	0.8598	3.8167	0.1140	0.0500	0.2221	4.0388	5.9037	1.4617	0.2186
2	0.9312	4.1340	0.1102	0.1008	0.4475	4.5815	7.2064	1.5729	0.3298
3	0.9985	4.4325	0.1069	0.1633	0.7249	5.1574	8.6923	1.6854	0.4423
4	1.0607	4.7086	0.1040	0.2477	1.0994	5.8080	10.5377	1.8143	0.5712
5	1.1217	4.9793	0.1013	0.3543	1.5729	6.5522	12.7711	1.9491	0.7060
6	1.1823	5.2485	0.0989	0.4545	2.0175	7.2660	14.8871	2.0489	0.8057
7	1.2383	5.4973	0.0965	0.5162	2.2916	7.7889	16.2937	2.0919	0.8488

The static margin at 0 degree angle of attack was 15.67, 9.84, and 7.64 percent of the chord for Missions 1, 2 and 3, respectively. Static margin was considered positive if the neutral point was behind the center of gravity. This provides a nose down tendency to the plane, and this tendency gets stronger as angle of attack increases. When angle of attack goes below 0 degrees, static margin becomes negative. This causes the nose to pitch up until it returns to trim flight. The

reaction moments provided at each shown angle of attack will serve to return the plane to trim flight for positive and negative angles of attack, making the plane statically stable.

4.5 Mission Performance Estimate

The lift characteristics of our aircraft allow the team's plane to carry a 0.5 pound Medical Supply Cabinet during Mission 2, and 12 passengers during Mission 3. These payloads were chosen to reduce the risk of the team failing a mission due to not taking off within 20 feet. The specific takeoff distance for each mission will be explored further with the Weight and Balance of the final design, but each mission will be able to take off within the limitation with some distance to spare. The drag characteristics of our plane indicate that drag will match thrust at approximately 51.9 feet per second. For the plane's Mission 2 score, this will create a three lap time of 115.61 seconds. For Mission 3, the plane will complete 7 full laps within the 5 minute window. The propulsion battery capacity will be 3200 mAh. Our mission performance for all these parameters will be plugged into the scoring equations as a fraction of the best performing team.

5. Detail Design

5.1 Dimensional Parameters of Final Design

Table 16. Dimensional Parameters of Final Design

General Airframe		Fuselage	
Length	50.86 in	Body Shape	Slab-sided
Height	20.08 in	Length	48 in
Ground Clearance	6.2 in	Maximum Width	3.6 in
Horizontal Stabilizer		Maximum Height	6 in
Root Chord	9 in	Payload Size	3.6 x 12 in
Tip Chord	4.5 in	Wing	
Span	18 in	Airfoil	FX 60-100
Vertical Stabilizer		Span	60 in
Root Chord	7.8 in	MAC	12 in
Tip Chord	3.9 in	Flap Deflection	16°
Span	8.4 in	Angle of Incidence	6°

5.1.1 Fuselage Dimensional Parameters

The total fuselage length will be 48 inches and have a maximum cross-section of 3.6 x 6 inches for the main payload compartment. This compartment will be 12 inches long to accommodate both the payload for Mission 2 and a maximum number of 12 passengers for Mission 3. The avionics and crew compartments will both be 4 inches long, with the top surface of the fuselage sloping down approximately 24.5 degrees over the crew compartment to the nose, which will have a maximum cross-section of 3.6 x 4 inches.

5.1.2 Landing Gear Dimensional Parameters

The team opted for a tricycle landing gear configuration. This means the landing gear will be in two separate pieces: the front and rear landing gear. The front landing gear will be 12.33 inches ahead of the rear landing gear. The rear landing gear will provide 19.10 inches of separation between the wheels. Both the front and rear landing gear with wheels attached are approximately 6.20 inches tall, providing ample clearance for propeller operation. The front landing gear will be 7.48 inches from the plane's nose.
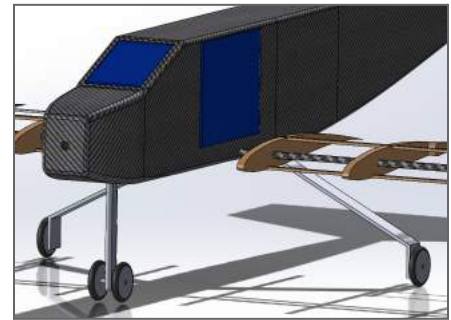

Figure 30. Landing Gear Design

5.1.3 Wing Dimensional Parameters

The airfoil and planform selection in the Preliminary Design section allowed the team to find the optimal dimensional parameters for the final wing design. For a rectangular planform, this meant choosing a wingspan and a chord length. The team decided to use the entire 5 feet of wingspan allotted by the rules. This will serve to increase aspect ratio, which will reduce induced drag. The team chose a chord length based on a wing area and coefficient of lift value that met the constraints of our takeoff distance. The wing will have flaperons that extend 3.61 feet along the span and 1/3 of the chord. This will allow the plane to create enough lift for takeoff with flaps deployed, then return to a lower drag state when in flight. The team analyzed wings with varying chord length and flap deflection in XFLR5 [5]. The team found the wing's coefficient of lift to be 1.140 with a 1 foot chord length, 16 degree of flap deflection and a 6-degree angle of incidence. The wing dimensions and coefficient of lift allow for a weight of 5.486 pounds to be lifted within 20 feet. The takeoff distance calculation accounts for the lower air density in Wichita, Kansas (Elevation of 1,303 feet above sea level). The static thrust of our motor-propeller combination (5.486-pound force) was also used in calculations using the takeoff distance equation [11].

5.1.4 Stabilizer Dimensional Parameters

With a wing area of 5 feet squared, mean aerodynamic chord of 1 foot, a wingspan of 5 feet, and a distance of 3 feet between the wing and stabilizer aerodynamic centers, the ideal horizontal and vertical stabilizer areas were found to be 0.8333 and 0.3333 feet squared respectively. The team found that a root chord of 0.75 feet, tip chord of 0.375 feet, and a

span of 1.5 feet for the horizontal stabilizer satisfied the specifications defined above. A root chord of 0.65 feet, tip chord of 0.325 feet, and a span of 0.7 feet for the vertical stabilizer met our specifications.

5.2 Structural Characteristics

During inspection, judges will test if the wing has adequate structure by conducting a wing tip loading test. Specifically, structural integrity will be verified for a 2.5g load case. The expected plane weight is 5 pounds, but a factor of safety of 1.2 was used in structural design, resulting in a 6-pound load for 1g. The structure was also designed to withstand a 3g load case, as the rules stipulate the load will be, "'roughly' equivalent to a 2.5g load case" [1]. This led to an 18-pound concentrated load on the center of the structure. The reaction force will be 9 pounds at each wingtip. Figure 31 shows the final load case used in wing structural design. The maximum bending stress that developed was found using the internal moments and the geometry of varying rods and tubes, in accordance with equations (11) (12) and (13) [12]. This was then compared to the yield stress for each material. The weight of each was also taken into consideration. The ideal structural component will be able to withstand the wingtip load test at the lowest weight cost.

Bending Moment Diagram & Bending Stress for Rods

Weight ≈ 6lbf. A 3G load is 18 lbf, causing a 9lbf reaction at the wing tips.

$0in \leq x < 30in$

$^{+}\downarrow \Sigma F_y = 0 \therefore v - 9 = 0 \therefore v = 9lbf$

$\Sigma M = 0 \therefore M - 9x = 0 \therefore M = 9x \; lbf \cdot in$

Bending Stress: $\sigma = \dfrac{My}{I}$ (11)

For a rod: $I = \dfrac{\pi d^4}{64}, \; y = \dfrac{d}{2}$

$\sigma = \dfrac{M\left(\frac{d}{2}\right)}{\frac{\pi d^3}{32}\left(\frac{d}{2}\right)} = \dfrac{M}{\left(\frac{\pi d^3}{2}\right)} = \dfrac{32M}{\pi d^3}$ (12)

$30in \leq x < 60in$

$^{+}\downarrow \Sigma F_y = 0 \therefore v + 18 - 9 = 0 \therefore v = -9lbf$

$\Sigma M = 0 \therefore M - 9x + 18(x - 30) = 0 \therefore M = -9x + 540 \; lbf \cdot in$

For a tube: $I = \dfrac{\pi\left(d_0^4 - d_i^4\right)}{64}, \; y = \dfrac{d_0}{2}, \; \sigma = \dfrac{My}{I} = \dfrac{M\frac{d_0}{2}}{\pi\left(d_0^4 - d_i^4\right)} = \dfrac{32M \, d_0}{\pi\left(d_0^4 - d_i^4\right)}$ (13)
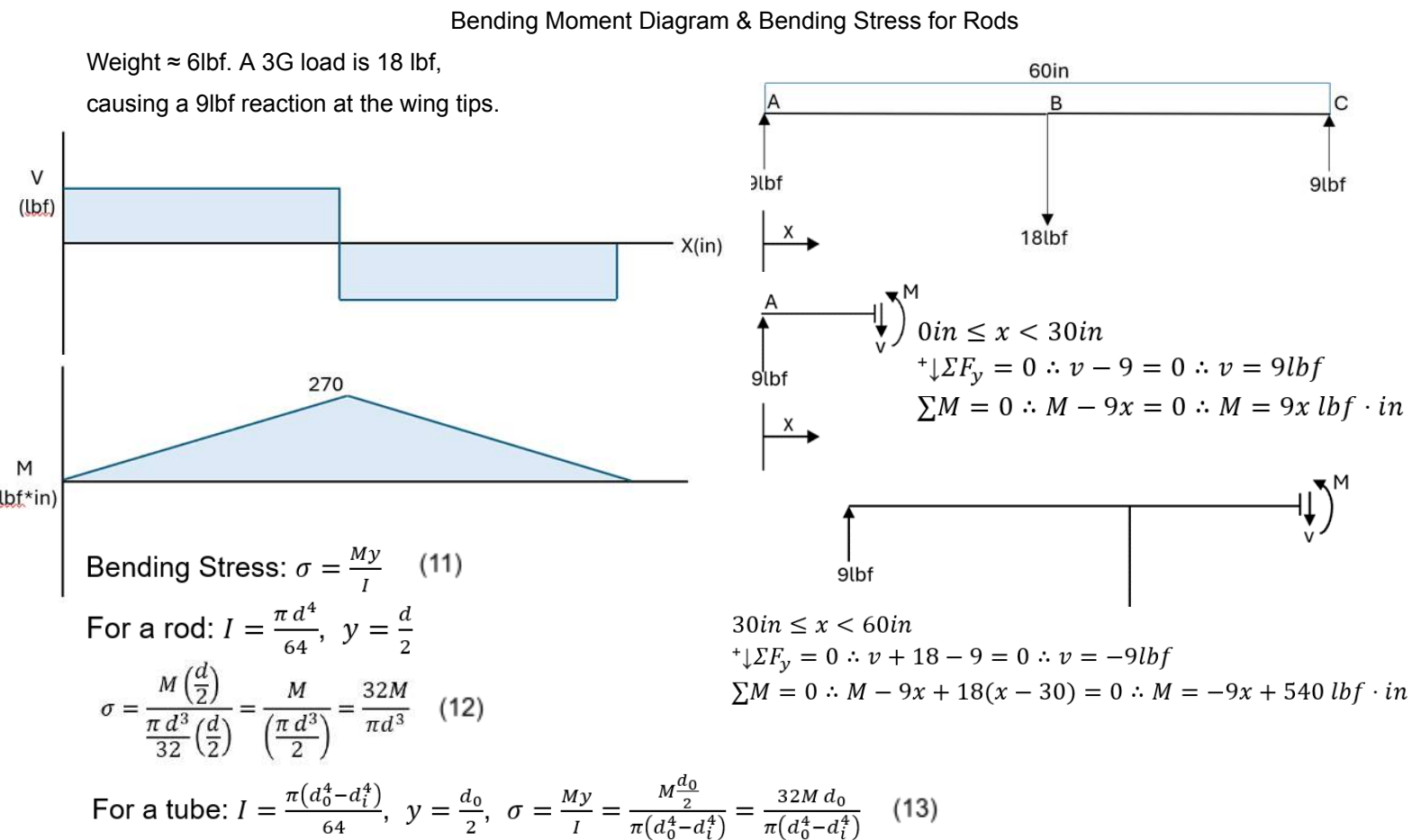
Figure 31. Analysis of Wing Structure for 3g Load Case

The bending stress due to this load was solved in rods and tubes composed of aluminum and carbon fiber. The potential components for use in the wing structure were found using McMaster-Carr [13]. Out of the aluminum and carbon fiber rods and tubes considered, the ideal structural component was found to be a carbon fiber tube with an outer diameter of 0.314 inches and an inner diameter of 0.236 inches. This tube reaches a bending stress of 130.5 ksi in these load conditions. Carbon fiber has a yield strength of 362.6 ksi, so this structural component will readily handle the load. The tube will have a weight of 0.1971 pounds. A maximum displacement of 3.438 inches was solved by using the maximum displacement equation (14) for a simply supported beam with a concentrated load at its middle [14]. Due to the variability in carbon fiber composition and quality, the team is confident in their decision to have such generous factors of safety in their calculations. The structure may be considered oversized, as the load case only reaches a third of the yield strength. However, the chosen tube was the smallest size available after a jump in wall thickness. The tubes with the smaller wall thickness than the one selected could not handle the loads present in the wingtip load test. Out of the tubes considered, the one selected is the lightest tube that can handle the loads present during structural verification.

The results of the displacement equation were verified using Ansys Static Structural Finite Element Analysis [3]. The performance of our chosen tube could not be verified due to the limitations of the material library provided by Ansys, but the validity of our analysis techniques were verified using an aluminum rod as a test case. The Ansys Finite Element Analysis of this test case can be seen in Figures 32 and 33. The team recognizes that the elimination of this analysis method makes physical testing of the carbon fiber tube necessary to ensure the structural integrity of the wing. Table 17 summarizes the results for each analysis method in the aluminum rod test case.

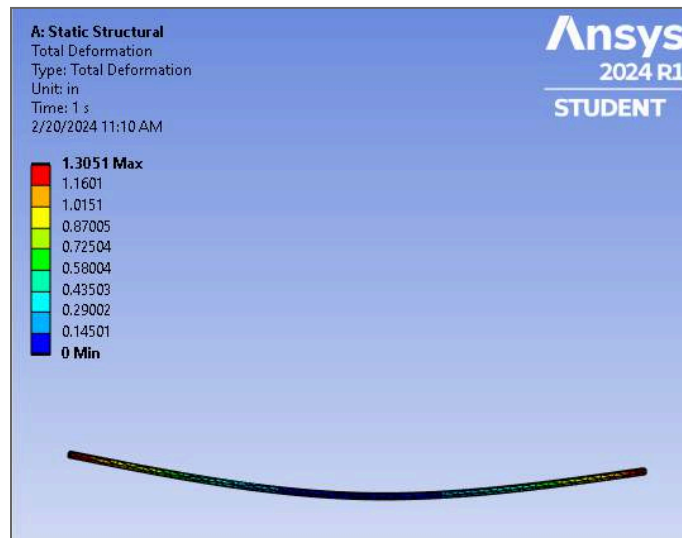$$\delta_{max} = \frac{PL^3}{48EI} \quad (14)$$

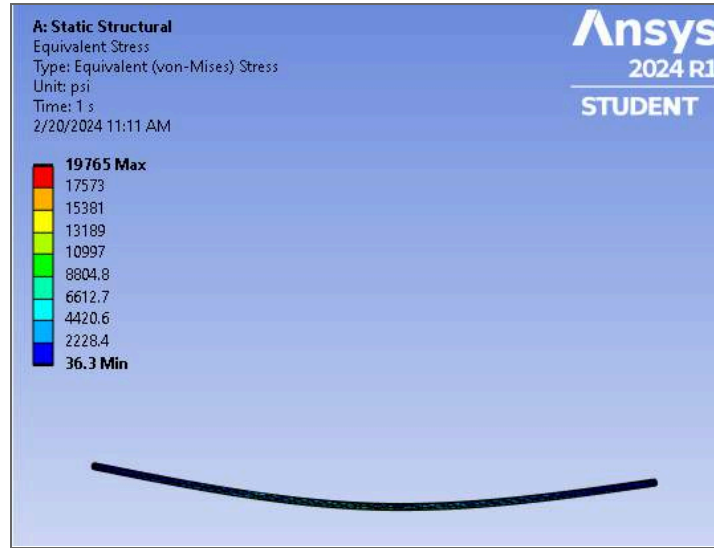Figure 32. Displacement of Loaded Rod Using Ansys Static Structural

Figure 33. Stress in Loaded Rod using Ansys Static Structural

Table 17. Summary of Results for Structural Analysis Methods

Analysis Method	Displacement (in)	Maximum Stress (psi)
Ansys	1.305	19765
Hand Calculation	1.351	22002
Physical Testing	1.375	

Based on the yield and ultimate strength of carbon fiber, calculations of the speed at which our wing structure will yield and fail were performed. The team found that a freestream velocity of 60.9 miles per hour (89.3 feet per second) will produce a load factor of 8.3 and will cause the wing structure to yield. A freestream velocity of 77.0 miles per hour (112.9 feet per second) will produce a load factor of 13.3 and will cause structural failure.

The wing ribs will be composed of 0.375-inch-thick balsa for applying the Ultracote covering. Additional structure and Ultracote bonding will be provided by 0.25x0.125-inch balsa sticks. 1/8th inch diameter aluminum rods will be used to support the flaperons.

5.2.1 Detailed Fuselage Structure

The fuselage is a carbon fiber monocoque with the forward and aft fuselage sections split into two to allow the aft section to fold vertically over the top of the main fuselage. The team opted for a folding fuselage design to comply with the 2.5 feet wide parking space rule due to its manufacturing simplicity and concerns regarding the structural characteristics of a folding wing. The back of the main fuselage has two hinges on top of the aircraft made from forged carbon fiber which will permit the vertical hinging motion required. The fuselage also features two hatches to load the payload. On the left side of the passenger compartment is a 6-inch wide hatch which will be used to load the EMTs, the patient on the gurney, the

Medical Supply Cabinet, passengers, and the floor inserts for Missions 2 and 3. Secondly, there is a top hatch above the two crew members so that they can quickly be dropped into place during each mission's timed aircraft reconfiguration. Per the rules, a solid bulkhead separates the two payload compartments. As a result of the aerodynamics case study, the aft section of the fuselage features a streamlined rounded taper to minimize drag. Additionally, the frontal area was streamlined, with the nose converging into a smaller cross-section for the motor mount, and all of the edges filleted to reduce sharp edges.

5.3 Systems and Sub-Systems

5.3.1 Landing Gear

The final landing gear design is a tricycle landing gear made from unidirectional forged carbon fiber components. The team opted out of using steerable front landing gear because it would add complexity of manufacturing and has more possible failure points. The tricycle landing gear was chosen due to ease of manufacturing, ease of take-off and landing, and they reduce the likelihood of a ground loop. Both landing gears will be bolted to the fuselage. Specifically, each wheel will be connected to the fuselage by a steel bolt and nut to the carbon fiber components.

FEA analysis was done on a close version of what will end up in the final design. The landing gear is going to be carbon fiber, however Solidworks does not have data regarding carbon fiber. Aluminum 6063-T4 was analyzed in the simulation. The simulation tested 25 pounds on top of the landing gear where the fuselage will be held. The weight is roughly equal to 3x the plane's total weight. The 25 pound force simulates a hard landing.
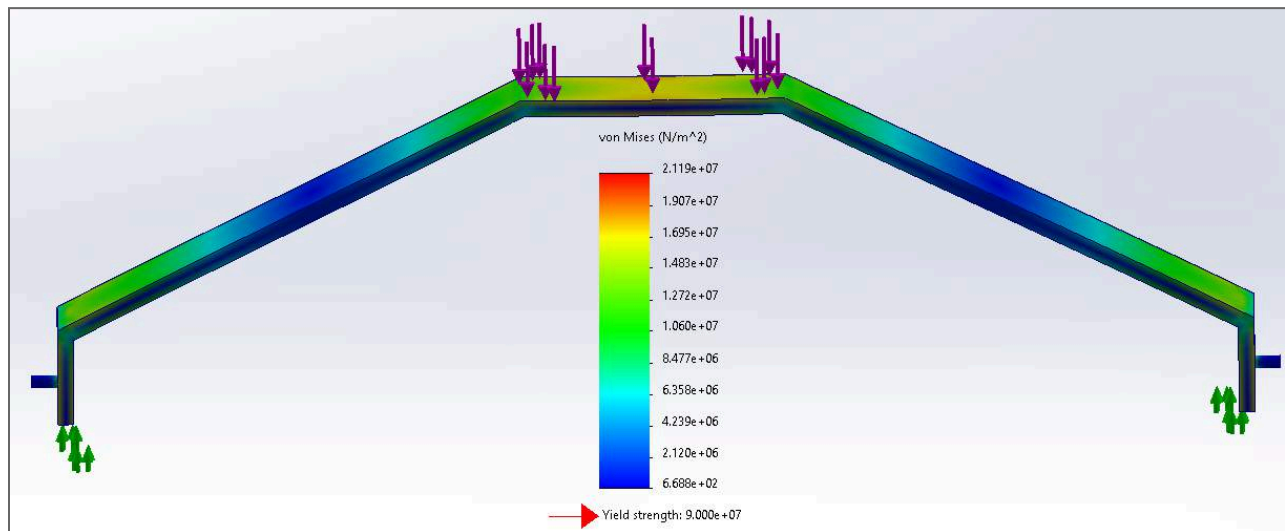

Figure 34. Ansys Static Structural Analysis for Landing Gear

5.3.2 Propulsion System

The propulsion for the system uses a Flysky 2826C V2 kv = 750 motor with a 13 x 11 APC propeller. The motor is mounted to the front face of the fuselage. The motor is connected to a 50 Amp ESC, which is sent digital signals from the receiver to control the throttle of the motor. The ESC is connected to the 3200 mAh battery that powers the propulsion system.

5.3.3 Cargo Deployment System

The main overall system for loading and unloading cargo will be loading the plane through the 6 inch wide hatch on the side of the aircraft. The interior of the plane utilizes a railing system on the sides of the fuselage for cargo. On the interior of the left and right sides of the interior are 2 guide rails on each side that span the length of the forward fuselage. The cutout slides across the rails and slides in the inside of the plane to make room for different configurations. There can only be a maximum 5.5 inch cutouts within the cargo area of the plane at a time along with the top loading pilot cutout. The pilot section of the aircraft is separated from the cargo by a bulkhead. Mission 1's configuration can be seen in Figure 35. Only the two pilots are in the pilot section of the aircraft.
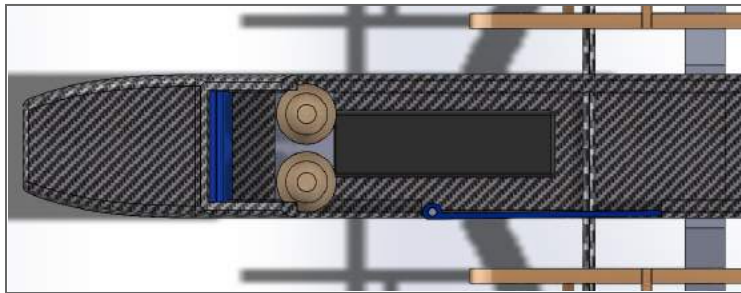

Figure 35. Mission 1 Payload Configuration

Mission 2's configuration can be seen in Figure 36. The two pilots are in the pilot section of the aircraft along with 2 crew members, a patient, and medical supply cabinet inside the cargo area.
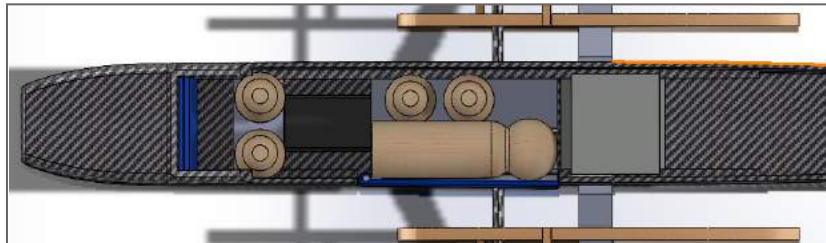

Figure 36. Mission 2 Payload Configuration

Mission 3's configuration can be seen in Figure 37. The two pilots are in the pilot section of the aircraft along with 12 passengers.

Figure 37. Mission 3 Payload Configuration

5.4 Weight and Balance

The team used Prototype 3 very extensively when analyzing the weight and balance of the final design. The effects of each component on balance was measured using the distance of each component's center of mass from the tip of the plane's nose and the weight of each component. The team found the moment about the nose tip caused by each component, then divided the sum of these moments by the calculated total weight. This gave the distance of the plane's center of mass from the tip of the nose. Many components and their locations within Prototype 3 will remain largely unchanged when creating the final design, so it was easy to physically measure their effects on weight and balance. Major components, such as the fuselage and the wing, cannot be measured directly yet, so the team found the weight and center of mass of these components using the "Mass Properties" feature in SolidWorks [15]. The team also ensured to assign the correct material to each component before using this feature. Table 18 shows the measured weight of each component.

Table 18. Component Weights

Component	Weight (lbf)
Propulsion Battery	0.525
Servo Battery	0.18125
Motor	0.4125
Propeller	0.10625
Nose cone	0.1
Fuselage	1
Insert	0.1
Crew Member	0.0875
Patient	0.3
Front Landing Gear	0.125
Rear Landing Gear	0.25
Wing	0.5
Wing Servos	0.008825608
Tail	0.2
Tail Servos	0.025
Music Wire (3-foot section)	0.125
Landing Gear Tire	0.025

With each component weighed, the team was able to find the weight and balance characteristics of each mission, as well as the weight and balance of the plane when empty. Table 19 shows the weight and balance for the empty plane, while Tables 20, 21 and 22 show the weight and balance tables for Missions 1, 2 and 3, respectively.

Table 19. Weight and Balance for Empty Plane

Component	Weight (lbf)	Distance from Nose Tip (ft)	Moment (lbf*ft)
Battery	0.5250	0.8333	0.4375
Servo Battery	0.1813	0.5000	0.0906
Motor	0.4125	0.0833	0.0344
Propeller	0.1063	0.0833	0.0089
Nose cone	0.1000	0.0833	0.0083
Fuselage	1.0000	1.5000	1.5000
Front Landing Gear	0.1250	0.6667	0.0833
Front Landing Gear Wheel	0.0250	0.6667	0.0167
Rear Landing Gear	0.2500	2.0000	0.5000
Rear Landing Gear Wheels	0.0500	2.0000	0.1000
Wing	0.5000	1.2000	0.6000
Wing Servos	0.0177	1.2000	0.0212
Tail	0.1200	3.5000	0.4200
Tail Servos	0.0250	3.5000	0.0875

Table 20. Weight and Balance for Mission 1

Component	Weight (lbf)	Distance from Nose Tip (ft)	Moment (lbf*ft)
Battery	0.5250	0.8333	0.4375
Servo Battery	0.1813	0.5000	0.0906
Motor	0.4125	0.0833	0.0344
Propeller	0.1063	0.0833	0.0089
Nose cone	0.1000	0.0833	0.0083
Fuselage	1.0000	1.5000	1.5000
Insert	0.2000	1.0000	0.2000
Crew	0.1750	0.7917	0.1385
Front Landing Gear	0.1250	0.6667	0.0833
Front Landing Gear Wheel	0.0250	0.6667	0.0167
Rear Landing Gear	0.2500	2.0000	0.5000
Rear Landing Gear Wheels	0.0500	2.0000	0.1000
Wing	0.5000	1.2000	0.6000
Wing Servos	0.0177	1.2000	0.0212
Tail	0.1200	3.5000	0.4200
Tail Servos	0.0250	3.5000	0.0875

Table 21. Weight and Balance for Mission 2

Component	Weight (lbf)	Distance from Nose Tip (ft)	Moment (lbf*ft)
Battery	0.5250	0.8333	0.4375
Servo Battery	0.1813	0.5000	0.0906
Motor	0.4125	0.0833	0.0344
Propeller	0.1063	0.0833	0.0089
Nose cone	0.1000	0.0833	0.0083
Fuselage	1.0000	1.5000	1.5000
Insert	0.2000	1.0000	0.2000
Crew	0.1750	0.7917	0.1385
Front Landing Gear	0.1250	0.6667	0.0833
Front Landing Gear Wheel	0.0250	0.6667	0.0167
Rear Landing Gear	0.2500	2.0000	0.5000
Rear Landing Gear Wheel	0.0500	2.0000	0.1000
Wing	0.5000	1.2000	0.6000
Wing Servos	0.0177	1.2000	0.0212
Tail	0.1200	3.5000	0.4200
Tail Servos	0.0250	3.5000	0.0875
EMT1	0.0875	1.2000	0.1050
EMT2	0.0875	1.4000	0.1225
Patient	0.3000	1.3000	0.3900
Medical Supply Cabinet	0.5000	1.6000	0.8000

Table 22. Weight and Balance for Mission 3

Component	Weight (lbf)	Distance from Nose Tip (ft)	Moment (lbf*ft)
Battery	0.5250	0.8333	0.4375
Servo Battery	0.1813	0.5000	0.0906
Motor	0.4125	0.0833	0.0344
Propeller	0.1063	0.0833	0.0089
Nose cone	0.1000	0.0833	0.0083
Fuselage	1.0000	1.5000	1.5000
Insert	0.2000	1.0000	0.2000
Crew	0.1750	0.7917	0.1385
Front Landing Gear	0.0875	1.2000	0.1050
Front Landing Gear Wheel	0.0875	1.2000	0.1050
Rear Landing Gear	0.0875	1.4000	0.1225
Rear Landing Gear Wheels	0.0875	1.4000	0.1225
Wing	0.0875	1.6000	0.1400
Wing Servos	0.0875	1.6000	0.1400
Tail	0.0875	1.8000	0.1575
Tail Servos	0.0875	1.8000	0.1575
Passenger 1	0.0875	2.0000	0.1750
Passenger 2	0.0875	2.0000	0.1750
Passenger 3	0.0875	2.2000	0.1925
Passenger 4	0.0875	2.2000	0.1925
Passenger 5	0.1250	0.6667	0.0833
Passenger 6	0.0250	0.6667	0.0167
Passenger 7	0.2500	2.0000	0.5000
Passenger 8	0.0500	2.0000	0.1000
Passenger 9	0.5000	1.2000	0.6000
Passenger 10	0.0177	1.2000	0.0212
Passenger 11	0.1200	3.5000	0.4200
Passenger 12	0.0250	3.5000	0.0875

Using the weight and balance tables presented for each mission, the gross takeoff weight and location of the center of gravity for each mission could be determined. Table 23 shows the gross takeoff weight, location of the center of gravity relative to the tip of the nose and projected takeoff distance for each mission.

Table 23. Gross Takeoff Weight, Center of Gravity Location, and Takeoff Distance for All Configurations

Mission	Gross Takeoff Weight (lbf)	Location of Center of Gravity Relative to Nose Tip (ft)	Takeoff Distance (ft)
Empty	3.438	1.137	N/A
Mission 1	3.893	1.163	10.070
Mission 2	4.868	1.221	15.747
Mission 3	4.768	1.243	15.107

The gross takeoff weight of our design met the takeoff distance limitation of 20 feet for all three missions. These results matched our previously calculated weight limitation of 5.486 pounds for a takeoff distance of 20 feet.

5.5 Flight Performance

Based on data from previous prototypes, the final competition plane will fly faster than 30 miles per hour. The propulsion power will last the duration of the 5 minute flight. The take off distance will be less than 20 feet and have a mean lap time less than 50 seconds.

5.6 Drawing Package

The 4 drawings composed in Solidworks show the configurations, structural arrangement, systems layout/ location, and payload accommodation.
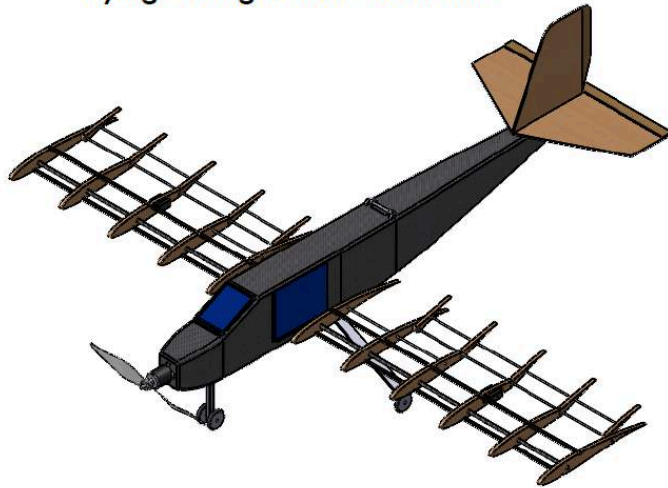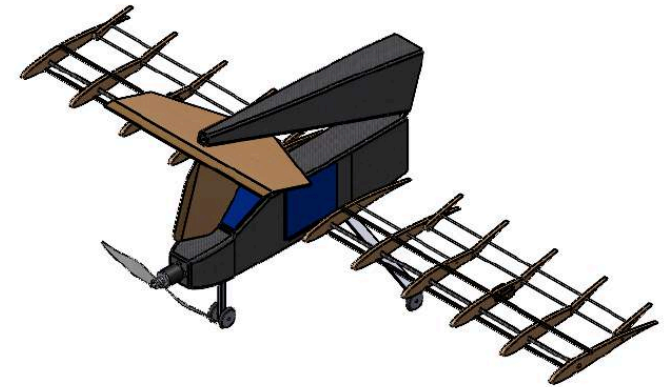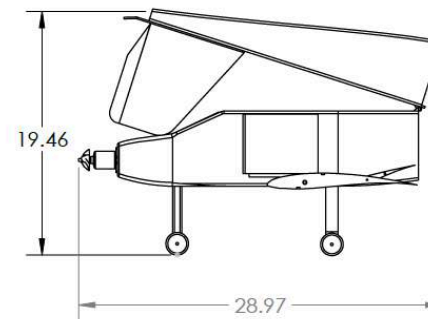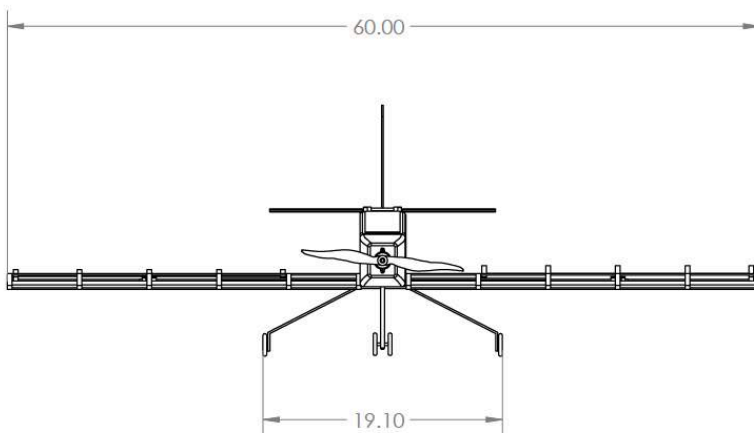
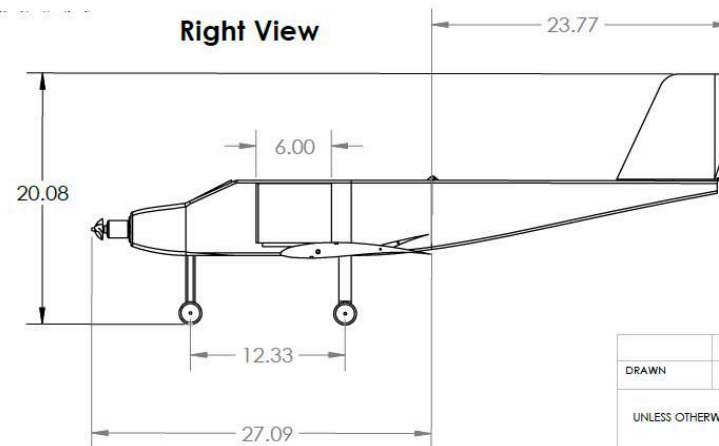**Flying Configuration - Isometric**

Parking Configuration - Isometric

B

Parking Configuration - Right view

19.46

28.97

Front View

60.00

19.10

Right View

23.77

6.00

20.08

12.33

27.09

A

	NAME	DATE
DRAWN	C.O	2-20-24

University of West Florida

TITLE:

Configurations

UNLESS OTHERWISE SPECIFIED:

DIMENSIONS ARE IN INCHES
TOLERANCES:
TWO PLACE DECIMAL ± .02

SIZE	DWG. NO.		REV
B	**Final**		**A**

SCALE: 10 | WEIGHT: | SHEET 1 OF 1

Balsa Airfoil

Carbon Fiber Hinge

Balsa Vertical Stabilizer

Balsa Horizontal Stabilizer

Pilot Hatch

Carbon Fiber Hinge rod

Rear Carbon Fiber Fuselage

Front Carbon Fiber Fuselage

Dualsky DC Motor

Mission 3 inserts with passengers

Aluminum Rod

13 x 11 in Propeller

Carbon Fiver Tube

Pilots

Carbon Fiber landing gear

Foam Wheels

Side Hatch
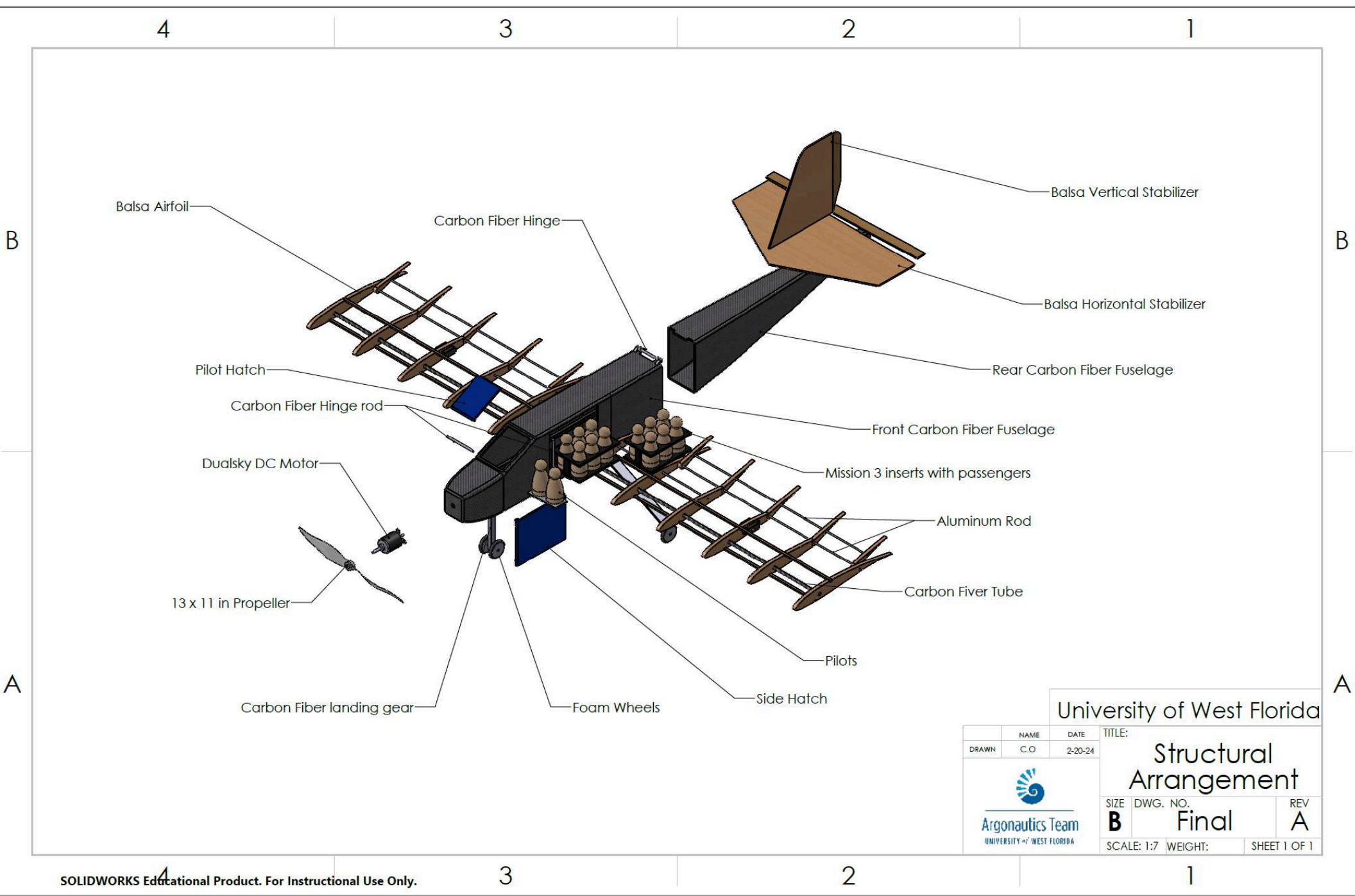
University of West Florida

	NAME	DATE	TITLE:
DRAWN	C.O	2-20-24	Structural Arrangement

Argonautics Team
UNIVERSITY of WEST FLORIDA

SIZE	DWG. NO.		REV
B	Final		A
SCALE: 1:7	WEIGHT:		SHEET 1 OF 1

Top View

Electronics and Propulsion
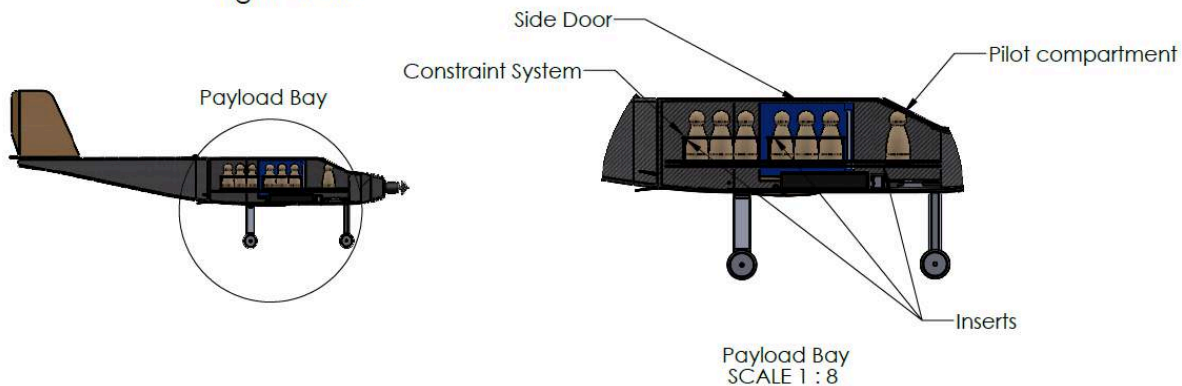
Servo

Motor

13 x 11 Propeller

Receiver Battery

50 Amp ESC

Propulsion Battery

Electronics and Propulsion
SCALE 1 : 8

Isometric View

Pivoting Mechanism

Right View

Payload Bay

Side Door

Constraint System

Pilot compartment

Inserts

Payload Bay
SCALE 1 : 8

	NAME	DATE	TITLE:
DRAWN	C.O	2-20-24	

University of West Florida

Systems
Layout/Location

UNLESS OTHERWISE SPECIFIED:

DIMENSIONS ARE IN INCHES

TOLERANCES:
TWO PLACE DECIMAL   ±.02

SIZE	DWG. NO.	REV
B	Final	A

SCALE: 1:8   WEIGHT: SHEET 1 OF 1
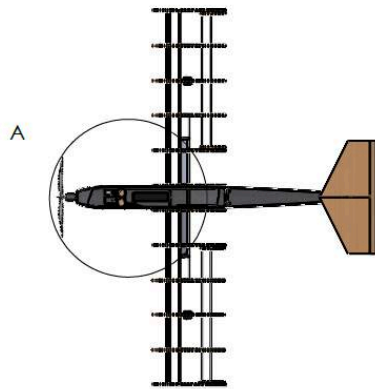
Mission 1

Mission 2
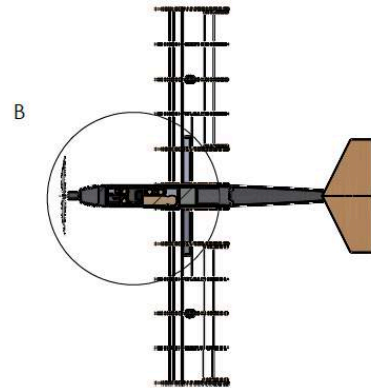
Mission 3
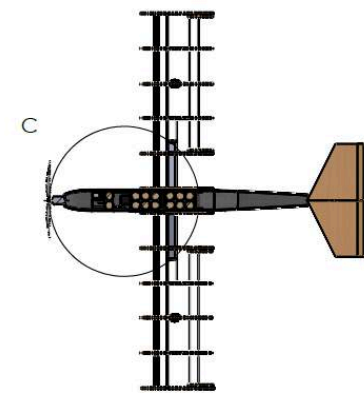
A

B
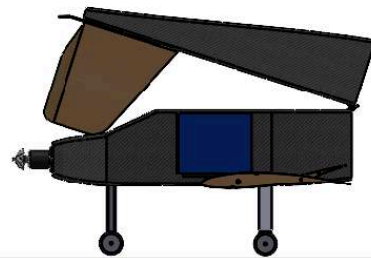
C

B

A

Pilots

A
SCALE 1 : 8

Medical
Supply
Cabinet

Patient

B
SCALE 1 : 8

12 x Passengers

C
SCALE 1 : 8

Side View
Parking Configuration
No Crew or Cargo

University of West Florida

	NAME	DATE	TITLE:
DRAWN	C.O	2-20-24	Payload Accommodation

UNLESS OTHERWISE SPECIFIED:

DIMENSIONS ARE IN INCHES

SIZE	DWG. NO.		REV
B	Final		A

SCALE: 1:16 | WEIGHT: | SHEET 1 OF 1

6. Manufacturing Plan

The general timeline in Figure 38 shows the schedule to have each prototype built and flown. The final designed aircraft should be finished manufacturing a month before the competition date.

Figure 38: Manufacturing Milestone Chart

6.1 Manufacturing Processes Investigated and Selection Process and Results.

6.1.1 Additive Manufacturing

Additive Manufacturing is very suitable as an inexpensive means of manufacturing parts and molds used in the construction of models, both rapid and final. Due to the nature of computer-aided-design, very complex parts, molds and models can be produced with great precision and property variability depending on the material used.

6.1.2 Laser Cutting

Laser Cutting is a staple within the RC aircraft community. Inherently fast due to its automated nature laser cutting has the demerit of being potentially wasteful when dealing with post-processed scraps. Overall, laser cutting is still seen as a go to for rapid reproduction of parts and models.

6.1.3 Composite Molding

Composite molding is a very appealing manufacturing process for use in the aeronautic industry. In its complexity, advantages such as its great strength and inherently lightweight properties makes composite molding highly sought after. Additionally, the process is very time consuming, the durability of composite materials in response to sudden impacts is very commendable. However, the direction of the fiber grain can influence the yield strength of the subsequent part/material.

6.2 Process Selection for Major Component Manufacture.

6.2.1 Wing Ribs

The team has decided to laser cut our balsa ribs for wing construction. In previous design competitions, the team has used balsa for fuselage components. The team did not have access to a laser cutter and had to pay a company to do it. This was a major expense for the team, so our use of balsa was limited to fuselage components. The components of the wing used in conjunction with this fuselage were 3D printed with PLA filament. The airfoil used in this wing had very dramatic changes in thickness. When applying Ultracote to the wing, the hot iron would deform the thin trailing edge of the ribs. Also, the Ultracote did not adhere as well to the PLA as it did to balsa. This year, the team has access to free laser

cutting services through the university. This will majorly reduce the costs of using balsa for plane components. Balsa ribs were chosen for manufacturing the wing because it is easier to construct with and can be done for no cost.

6.2.2 Fuselage

The fuselage will be constructed from composite materials via molded vacuum bag lamination. The composite molding process is experimental but lucrative for ensuring that the fuselage is both lightweight and durable during the plane's multiple operations. Carbon Fiber will be used due to the high risk nature of structural integrity and potential misalignment stresses from the folding fuselage design. The use of Carbon Fiber is experimental as it is the team's first year manufacturing parts for application in the aerospace field. Objectively, negative molds of the front and rear fuselage will be 3D printed with PLA and then layered in Carbon Fiber laminate before pressurized in a vacuum bag. Splitting the fuselage design vertically, the molds will total as five pieces including the door/hatch. After the carbon fiber is curated the four fuselage halves will be assembled with epoxy fixings and screw attached hinges.

6.2.3 Empennage

The empennage will be constructed using Balsa wood. The Balsa wood will be ordered en masse and processed through the university's laser cutting services. For ease of assembly, the Horizontal Stabilizer will be cut with appropriately sized holes that will match to the corresponding insert features on the Vertical Stabilizer. Subsequently, screw holes will be drilled near the edges of the stabilizers, rudders and elevators before being connected via screws for the hinges and epoxy for the control servos. Together, the Vertical and Horizontal Stabilizer will be combined using an epoxy resin as a binder. Lastly, the empennage will be affixed to the rear fuselage using epoxy resin. Throughout the process appropriate management of epoxy is paramount to the construction of the plane.

6.2.4 Landing Gear

The landing gear will be constructed from carbon fiber composites via vacuum bag lamination. In previous years, the landing gear was a critical component of analysis when creating and testing prototypes, thus carbon fiber was chosen to ensure the part is lightweight and durable. Firstly, a negative mold of the landing gear will be 3D printed in PLA filament using a SolidWorks model. The mold consists of two pieces with a collinear through hole for the attachment of the wheel and a mounting surface for completed landing gear to be affixed to the bottom of the front fuselage via epoxy resin. Carbon fiber laminate will then be vacuum bagged onto the mold for curation. Subsequently, the carbon fiber will be aligned together using epoxy resin and then affixed with the appropriate wheel and mounting assembly.

7. Testing Plan

The overall testing plan is to do small controlled tests over a period of time to narrow down the best fit for the selection of structural and electrical components needed for the final plane. Based on the data collected from the tests the final competition aircraft design is authenticated.

7.1 Schedule and Objectives

To conduct all tests in an efficient manner, the team created a schedule for different tests. The main goal of these tests are to determine if a component can be used for the competition plane and show real world testing of the materials being used.

Table 24. Testing Plans

Date	Test	Objectives
9-15-23	Electronic Systems	Ensure electronics work when connected
10-1-23	Structure	Ensure material will be strong enough for plane
11-1-23	Static Thrust	Collect thrust data of motor and propeller with no air speed
11-1-23	Dynamic Thrust	Collect thrust data of motor and propeller with air speed
11-7-23	Radio Failsafe	Ensure failsafe works
11-7-23	Radio Range	Collect maximum radio range
11-18-23	Flight(Prototype 1)	Perform flight test
11-18-23	Ground Handling	Ensure the plane can taxi on the ground
11-28-23	Take Off Distance	Ensure the plane takes off within 20 ft
12-1-23	Electronics Systems Duration	Ensures 5-minute flight time
12-7-23	Landing Gear Shock	Proves landing gear can withstand flight
12-13-23	Flight Control Handling	Trim prototype 1
12-13-23	Flight (Prototype 2)	Perform a flight test
12-13-23	Tip Loading	Ensure wings can withstand flight
12-13-23	Assembly Time	Collected data on time for mission configurations swap
12-13-23	Cruise Performance	Gathered data about flight characteristics
1-20-24	Flight (Prototype 3)	Perform a flight test

7.2 Ground Testing

Table 25. Ground Testing Purposes and Methods

Ground Testing	Purpose	Method
Electronics systems	Ensure the electronics work as needed and will work for a duration of 5 min flight under load.	Connect all electronics to ensure everything works. Check the battery capacity at the start of the test and put all electronics under load for 5 min. Check battery capacity again to ensure the plane will be able to fly for 5 min.
Landing Gear	Ensure landing gear will hold the weight of the plane during take off and landing.	Install landing gear on the fuselage and incrementally add weight up to maximum weight.
Static Thrust	Determine Static thrust from motor and propeller to be able to calculate take off distance.	Using a thrust stand, connect the motor and run at full throttle. This will test static thrust, current, and voltage.
Dynamic Thrust	Determine the dynamic thrust to determine the top speed.	Using a thrust stand inside of a wind tunnel, connect the motor and run at full throttle. This will test static thrust, current, and voltage.
Tip Loading	Ensure the plane can handle maximum load during flight.	Using a tip stand, place the plane on its wingtips on either side. Incrementally increase the weight.
Assembly Time	Ensure payload is able to be inserted into the plane and load/ unload the plane quickly.	Place the payload inside the plane and load the plane in different configurations.

7.2.1 Static and Dynamic Thrust Testing

The static thrust tests were applied to 2 different motor and propeller combinations.The 1st motor is a Cobra 3515/14 kv=950. The 2nd motor is a Flysky 2826C V2 kv=760. The cobra was tested to compare the data collected with the Flysky motor. The Flysky motor data was collected from eCalc [7] and was determined to be a motor for the final design. The data collected will be used to make estimates on the top speed of the aircraft, take-off distance, gross take off weight, and Amerage used by the motor/ propeller combination..
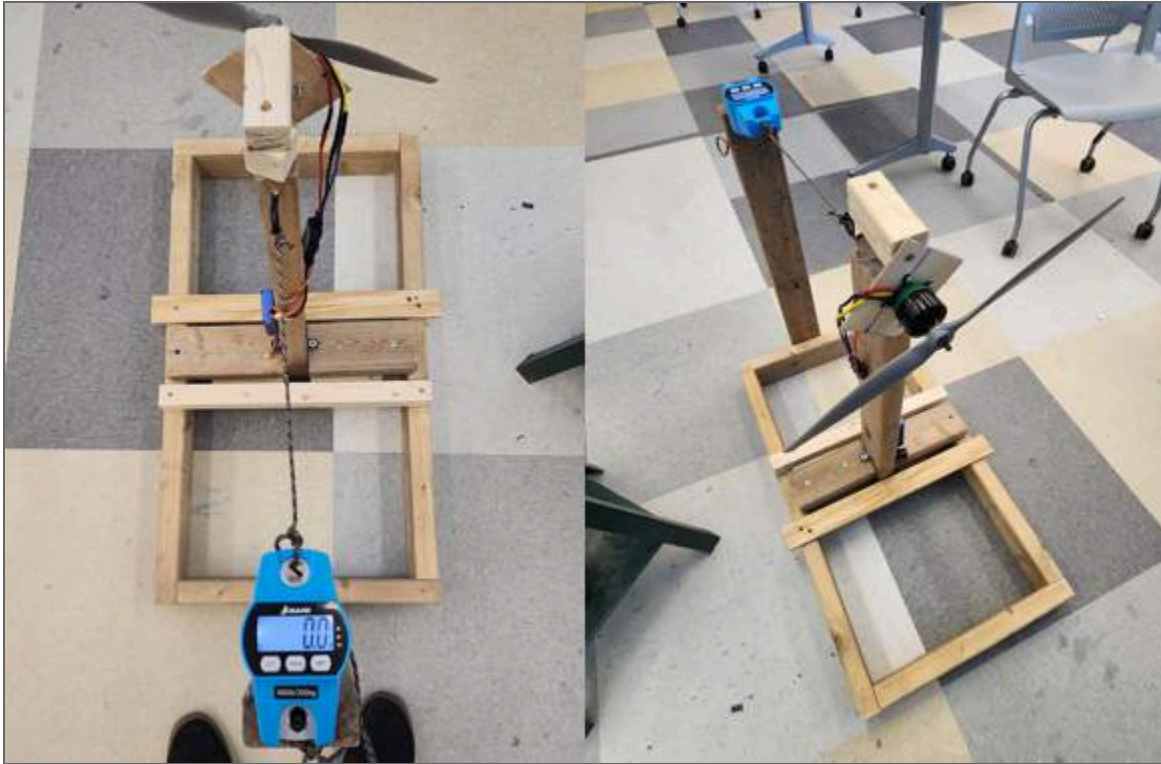

Figure 39. Thrust Testing Stand

7.2.2 Structural Testing

The team has created and verified testing methods to ensure the wing structure can pass the wingtip load test present in the safety inspection. The team verified structural integrity through Ansys Static Structural, hand calculations, and physical testing. The validity of the team's structural testing methods are demonstrated using our test stand and an aluminum rod of ½ inch diameter and 48 inch length. The rod was placed in our test stand with the top surface measuring at 6 inches on the yardstick as shown in Figure 39.

An 18 pound force load will be applied to the center of the rod, creating the loads shown in previous structural analysis sections.

Figure 40. Tip Testing Setup

7.3 Flight Testing

Flight testing consists of conducting tests while in flight. Major flight testing can be shown in Table 26.

Table 26. Flight Testing Purposes and Methods

Flight Testing	Purpose	Method
Radio Failsafe	Ensure failsafe activates when signal is lost.	Determine if fail safe activates after the transmitter loses radio signal with receiver.
Radio Range	Ensure the transmitter and receiver have proper range to complete flights.	Have the transmitter move away from the receiver until loss of signal.
Take off Distance prototype 1	Ensure the plane takes off within 20 feet.	Have the plane take off in the shortest distance possible.
Flight control Handling prototype 1	Ensure the plane has adequate control within the air.	The plane will gain altitude and will conduct different tests of control surfaces. The plane will be controlled to perform yaw turning, rolls in the lateral and longitudinal axes, and pitch.
Cruise Performance	Determine the battery drainage from 5 min of flight.	Determine the battery capacity right before flight. Then determine the battery capacity after 5 minutes of flight.
Ground Handling	Ensure the plane can maneuver while on the ground.	Taxi the plane around the runway.

Table 27. Prototype Images and Details

Argonautics Team UNIVERSITY *of* WEST FLORIDA	Aircraft	Details
Prototype 1		-Top mounted wing -Proof of concept
Prototype 2		-Bottom Mounted wing -Improves access to cargo -Better maneuverability
Prototype 3		-Best Maneuverability -Faster motor and propeller combination

7.4 Flight Checklist

Table 28. Flight Checklist

Before Power Up	
Main Battery Voltage	Must be > 16.5V (use multimeter or battery tester)
Receiver battery voltage	Must be > 7.2V (use multimeter or battery tester)
Visually inspect electronics	Dirt/moisture on boards, damaged/missing components
Transmitter Power	Must be > 30% (use onboard battery indicator)
Control Surfaces	Are pushrods bent or otherwise damaged?
Cabin/equipment	Are the passengers/equipment secure?
Tail latch	Is the folding tail mechanism secure?
Passenger door	Is the passenger door secure?
CG	Is the CG within limits? Perform wingtip holding test to determine CG.
Safety plug	Is the safety plug fully inserted?
After Power Up	
Control Surfaces	Do they move freely on command and hold their position?
Control surface direction	Do the control surfaces articulate in the correct direction? Right bank = right aileron up left aileron down. Etc.
Motor/Propeller	Do a run up. Is there excessive vibration of the motor/propeller assembly?
Landing gear	Does the gear wobble or otherwise behave abnormally during taxi?

Environment Check	
Wind direction	Choose which direction to take off into the wind if possible.
Plan climb and pattern	Find reference points to begin and execute turns in the pattern. (reference points should ideally be chosen before takeoff)
Plan landing	Always be thinking about how to perform a landing if necessary while the plane is in motion.

8. Performance Results

8.1 Subsystems

8.1.1 Propulsion Testing

To perform the dynamic thrust test the team had to find a way without using a wind tunnel due to the university not having a large enough wind tunnel test section. To gather some data on dynamic thrust the team put a fan that outputs 6500 ft^3/min and a laminar flow device in front of the fan. This was put in front of the motors/ propeller combinations and tested at a wind speed of 2.5 miles per hour.

Table 29. Static Thrust Testing Results

DC Motor @14.8V	Cobra 3515/14 kv = 950	Flysky 2826C V2 kv = 750
Propeller	15 x 4 E	13 x 11 APC
Static Thrust	3400	2400

Table 30. Dynamic Thrust Testing Results

DC Motor @14.8V	Cobra 3515/14 kv = 950	Flysky 2826C V2 kv = 750
Propeller	15 x 4 E	13 x 11 APC
Dynamic Thrust (g) @ 6.5 ft/s 2.5 mph	3500	2200

Regrettably, our methods for characterizing the dynamic thrust of our motor-propeller combinations did not appear to be valid. Thrust force should decrease as relative wind increases, but the test conducted using the Cobra motor seems to contradict this. The batteries were tested to determine the max amount of flight time the battery could produce with the amperage draw from the different motor and propeller combinations. The Spektrum 3200mAh propulsion battery lasted the longest with the Flysky motor at 370 seconds at ¾ throttle. The current draw calculated at full throttle from the Flysky

motor is 38 amps. Combining the Flysky motor and 3200 mAh battery the projected full throttle time period would be 305 seconds.

8.1.2 Structural Testing Results

The displacement of the top surface was noted using the yardstick as approximately 1.375 inches. The loaded rod and displacement can be seen in Figure 41.
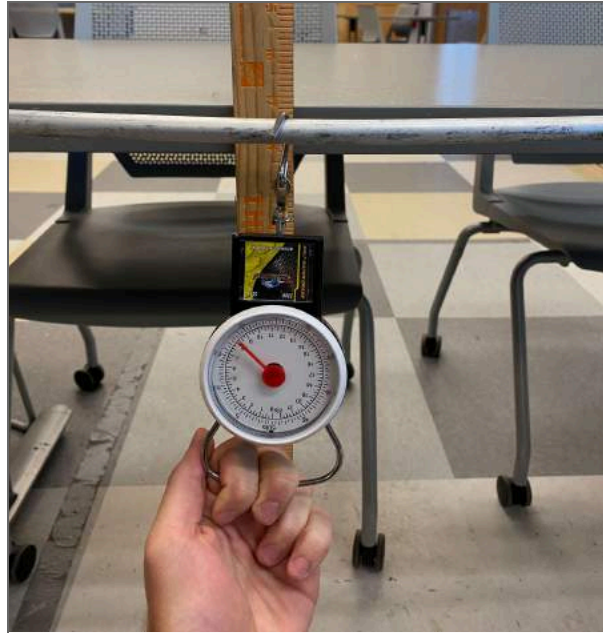

Figure 41. Aluminum Rod Sample Case, Loaded

The structural case presented verified results from both the Ansys Static Structural analysis and hand calculations, which found the maximum displacement to be 1.305 and 1.351 inches, respectively. This test case proved that our methods for the Tip Loading test are valid. This process will be repeated to ensure our chosen carbon fiber tube can withstand the load case presented. Physical testing will be very important for the carbon fiber tube, as the team could not find a matching material in the Ansys Engineering Data.

8.1.3 Test Flights

The team planned at the beginning of the competition semester to have 3 prototypes made and flown before competition.

The first prototype is a high wing, rectangular planform design with a Cobra 3515/14 kv=950 motor. This system utilized a 2200 mAh battery for about 2 minutes of flight time. Prototype 1 took off in less than 10 feet. The plane had an average lap time of 84 seconds.

Figure 42. Prototype 1

The 2nd prototype extended the fuselage and had a low wing design. The low wing design made the plane slightly less stable. The plane utilizes the same propulsion system as the 1st prototype. The take-off distance is very similar to

Prototype 1. The average lap time of the 2nd prototype was slightly less than the 1st prototype. The average lap time for the prototype is 70 seconds.

The 3rd prototype resembles the 2nd with its body sizing. The crew members can be placed in Prototype 3. When testing, the average time to switch between configurations is 35 seconds. The difference between Prototypes 1 and 2 vs 3 is that Prototype 3 has Ultracote across the entire surface of the plane reducing skin friction. The wing configuration changes from chocolate bar to a tapered wing. The third prototype uses a Flysky 2826C V2 kv = 750 motor with a 13 x 11 propeller. The motor is smaller than the Cobra motor, however it goes much faster. The plane took off within the 20 foot mark.

According to eCalc [7] the cobra motor and propeller combination top speed is 30 miles per hour. The Flysky motor and propeller combination top speed is 58 miles per hour. The average lap time for the flight is 50 seconds. The final prototype utilizes a 3200

Figure 43. Prototype 2

mAh battery to power its propulsion system. The servos used for the ailerons are responsive at high speeds. The plane flew very stable and was easily trimmed. The only downside for the plane is the tapered wing causes the wing to stall sooner than a conventional rectangular wing.

Figure 44. Prototype 3

The final aircraft is predicted to fly faster than 30 miles per hour. The take off distance will be less than 20 feet. The aircraft should have a 40 to 60 second lap time fully loaded. The batteries have been tested to show that the plane won't run out of power while in the air during the 5 minute flight time. The weight of the plane will be less than 5 pounds fully loaded. The plane can handle the tip loading test and will survive the harshest conditions in flight.

Bibliography

[1] AIAA, "2023-24 Design, Build, Fly Rules"

[2] "MATLAB" [ONLINE], R2023a, MathWorks

[3] "ANSYS Student" [ONLINE], 2024 R1, https://www.ansys.com/academic/students/ansys-student [Accessed 2024]

[4] "Airfoil Tools" [ONLINE], http://airfoiltools.com/ [Accessed 2024]

[5] "XFLR5" [ONLINE], v6.59, https://www.xflr5.tech/xflr5.htm [Accessed 2024]

[6] Raymer, D. P., "Aircraft Design: A Conceptual Approach", 6th ed., AIAA, 2018

[7] "eCalc" [ONLINE] Solution for All Markus Mueller [Accessed 2024]

[8] Gadd, C. *Servo Torque Calculator*. MN Scale & Giant Scale RC.

   https://www.mnbigbirds.com/Servo%20Torque%20Caculator.htm

[9] Weakley, L. *New Technology Weakley*. The Park Pilot, https://www.theparkpilot.org/new-technology-weakley

[10] Leishman, J. G., "Introduction to Aerospace Flight Vehicles",

   https://eaglepubs.erau.edu/introductiontoaerospaceflightvehicles/chapter/aircraft-stability-control/ [Accessed 2024]

[11] Anderson , J. D., "Introduction to Flight", 7th ed., McGraw-Hill Education, 2011

[12] Budynas, R. G. and Nisbett, K. J., "Shigley's Mechanical Engineering Design", 11th ed., McGraw-Hill Education 2020

[13] McMaster-Carr Supply Company [ONLINE], https://www.mcmaster.com/ [Accessed 2024]

[14] Kassamali, A., "Structural Analysis", 6th ed., Cengage, 2020

[15] "SOLIDWORKS" [ONLINE], Student Edition 2023, Dassault Systems